JAERI-M
82-022

PIPE RUPTURE TEST RESULTS; 4 INCH PIPE WHIP TEST UNDER BWR LOCA CONDITIONS —— OVERHANG LENGTH PARAMETER TESTS (RUN 5407, 5501, 5504, 5603)

March 1982

Ryoichi KURIHARA, Shuzo UEDA, Toshikuni ISOZAKI
Noriyuki MIYAZAKI, Rokuro KATO, Kazuo SAITO*
and Shohachiro MIYAZONO

日本原子力研究所
Japan Atomic Energy Research Institute

JAERI-M レポートは，日本原子力研究所が不定期に公刊している研究報告書です。

入手の問合わせは，日本原子力研究所技術情報部情報資料課（〒319—11 茨城県那珂郡東海村）あて，お申しこしください。なお，このほかに財団法人原子力弘済会資料センター（〒319—11 茨城県那珂郡東海村日本原子力研究所内）で複写による実費頒布をおこなっております。

JAERI-M reports are issued irregularly.

Inquiries about availability of the reports should be addressed to Information Section, Division of Technical Information, Japan Atomic Energy Research Institute, Tokai-mura, Naka-gun, Ibaraki-ken 319—11, Japan.

編集兼発行　日本原子力研究所
印　　刷　日立高速印刷株式会社

JAERI-M 82-022

Pipe Rupture Test Results; 4 inch Pipe Whip Test under BWR LOCA Conditions ——— Overhang Length Parameter Tests (RUN 5407, 5501, 5504, 5603)

Ryoichi KURIHARA, Shuzo UEDA, Toshikuni ISOZAKI
Noriyuki MIYAZAKI, Rokuro KATO, Kazuo SAITO *
and Shohachiro MIYAZONO

Division of Reactor Safety, Tokai Research Establishment, JAERI

(Received February 10, 1982)

Pipe whip tests or jet discharge tests have been performed in JAERI, which simulate the instantaneous circumferential guillotine break of primary coolant piping in nuclear power plants. This report summarizes the results of 4 inch pipe whip tests (RUN 5407, 5501, 5504, 5603), under BWR LOCA conditions, which were performed from 1979 to 1981. The test pressure was 6.8 MPa and test temperature 285 °C. In these tests clearance was kept constant at the value of 100 mm and overhang length were 250 mm, 400 mm, 550 mm and 1000 mm, respectively.

The main purpose of these tests was to investigate the effect of overhang length on pipe whip behavior. From the tests results, a shorter overhang length is recommended to minimize the deformation of the pipe and restraints.

Keywords;Pipe Whip,4 inch Test Pipe,Restraint,Overhang Length, LOCA, BWR Operating condition,Clearance,Residual Deformation

---

This work was performed under the contact between the Science and Technology Agency of Japan and JAERI to demonstrate the safety against pipe rupture of the primary coolant circuits in nuclear power plants.

*) Ishikawajima Harima Heavy Industries Co., Ltd.

JAERI－M 82－022

配管破断試験結果；BWR・LOCA 条件4インチ口径パイプホイップ試験 ── オーバーハング長さの効果

日本原子力研究所東海研究所安全工学部
栗原　良一・植田　脩三・磯崎　敏邦・宮崎　則幸
加藤　六郎・斎藤　和男*・宮園昭八郎

（１９８２年２月１０日受理）

日本原子力研究所では原子炉の一次冷却系配管が周方向に瞬時破断した場合を想定してパイプホイップ試験とジェット放出試験が実施されている。本報は１９７９年から１９８１年までに実施したＢＷＲ条件４インチ口径パイプホイップ試験（ＲＵＮ　５４０７，５５０１，５５０４，５６０３）の結果をまとめたものである。試験圧力は6.8ＭＰａ，試験温度は２８５℃である。これらの試験でクリアランスは１００mm一定とし，オーバーハング長さはそれぞれ２５０mm，４００mm，５５０mmおよび１０００mmに変えた。

試験の主な目的はパイプホイップ挙動におけるオーバーハング長さの影響を調べることである。試験結果からオーバーハング長さが短いほど配管およびレストレントの変形をより小さくすることが判明した。

本報は電源開発促進対策特別会計施行令に基づき，科学技術庁から日本原子力研究所への委託研究，配管信頼性実証試験の内，配管破断試験；BWR・LOCA条件4インチ口径パイプホイップ試験の結果をもとめたものである。

*）石川島播磨重工業（株）

CONTENTS

目　　次

1. INTRODUCTION

In the hypothetical pipe break accident in a light water reactor nuclear power plant, adequate protection against pipe movement (pipe whip) must be considered.[1] For this purpose various kinds of restraints are used in many nuclear plants in order to stop the pipe whip motion in nuclear piping systems. The restraints should be so located that the containment and the necessary safety systems are out of reach of a moving pipe section if a pipe break accident occurs.

A series of pipe rupture tests has been performed using FRPC-II*[2] in JAERI to demonstrate the safety of the primary coolant circuits in the event of pipe rupture, in nuclear power plants. Pipe whip tests are carried out to investigate the behavior of a pipe and restraints. This report summarizes the results of 4 inch pipe whip tests (RUN 5407, 5501, 5504, 5603) under BWR LOCA conditions (285 °C, 6.8 MPa), which were performed from 1979 to 1981.

Clearance and overhang length are considered as important basic parameters of the pipe whip test[3]. Clearance is the distance between a pipe and restraints, and overhang length is the distance from a setting point of its restraints to the free end of the pipe. A previous report[4] clarified the effect of clearance on pipe whip motion. The main purpose of these tests was to investigate the effect of overhang length on the pipe whip motion. In these tests, clearance was kept constant at the value of 100 mm and overhang lengths were 250 mm, 400 mm, 550 mm and 1000 mm.

---

* FRPC-II: Facilities for Reliability Study of Pressure Boundary Components-II

2. TEST PROCEDURE

2.1 Test Equipment

The profile of the testing system is shown in Fig.2.1. The volume of the pressure vessel is about 4 m^3. An auxiliary connecting pipe which reduces the diameter of the 8 inch nozzle to the diameter of the 4 inch test pipe is attached to the nozzle of the pressure vessel. The 4 inch test pipe is 4500 mm in length and is fixed by the pipe support so that the length of the test section is 3000 mm.

A detailed assembly of the test pipe and the restraint is shown in Fig.2.2. The test pipe is installed at the height of 1000 mm above the test bed. Four pipe whip restraints are set on the restraint support. In these tests, overhang length is taken as a test parameter. Clearance is the space between the pipe and restraints and the value is kept constant at 100 mm in these tests.

A view of the test system is shown in Photo 2.1. Hot water is circulated through the warming-up line which is attached to the elbow of the test pipe to keep the temperature of the test system uniform. A flexible tube is used as a part of the warming-up line to reduce its restriction to pipe whip motion.

The details of the restraint are shown in Fig.2.3. The restraint is composed of a U-bar, bearing plate, clevis, bracket and pin. The U-bar is made of Type 304 stainless steel and its diameter is 8 mm. The clevis is screwed to the end of the U-bar and is used for fine adjustment of clearance. The bearing plate made of carbon steel is attached to the inner side of the circular part of the U-bar. The purpose of this plate is to wrap around the test pipe to minimize pipe rebound. Restraint assemblies are pinned to the bracket which is set on the restraint support.

There were four restraints in these tests.

Details of the clevis are shown in Fig.2.4. The restraint force could not be measured by the standard type of clevis, so this type of clevis was designed in order to measure it. It was used in RUN 5501, RUN 5603 and RUN 5504.

The configuration of the welded type of rupture disk is shown in Fig.2.5. This rupture disk is butt-welded at the tip of the test pipe. This assembly was developed especially for the pipe whip test. A rupture disk was placed and welded between two segments of pipes. The weight of this assembly is lighter than a flange jointed type of rupture disk. Instantaneous pipe rupture is simulated by breaking this rupture disk using the electric arc method.

The chemical composition and mechanical properties of a pipe and restraints are summarized in Table 2.1. Both materials are Type 304 stainless steel.

2.2 Test Conditions

Test conditions for the four tests are summarized in Table 2.2. As can be seen from the table, the tests were conducted under the BWR operating conditions with 6.8 MPa pressure and 285 °C temperature of the primary coolant water. The temperature near the free end of pipe decreased a few degrees because of the heat radiation. RUN 5501, RUN 5407, RUN 5603 and RUN 5504 are the test numbers, and the overhang lengths are 250 mm, 400 mm, 550 mm and 1000 mm, respectively.

2.3 Measuring Items and Devices

Measuring items for each test are summarized in Table 2.3.1 and Table 2.3.2.

Measuring points around the pressure vessel are shown in Fig.2.6. The symbols XU, PU, WU and TU are the strain gages, pressure transducers, load cells and thermocouples, respectively.

The locations of measuring devices on the test pipe are shown in Fig.2.7.1 to Fig.2.7.4. High temperature strain gages were used and attached to the surface of the pipe by welding. Displacement measuring systems of XU 200 and XU 201 were the eddy current type and measured the transient displacement of the whipping pipe. The accelometers of XU 300, XU 301 and XU 302 were piezo type and attached to the locations shown in Fig.2.7. However, the displacement and acceleration of the pipe could not be obtained these tests because these devices were troubled by the high temperature atmosphere.

The locations of strain gages on the restraints are shown in Fig.2.8.1 to Fig.2.8.2. These strain gages were ordinary ones used at room temperature. For convenience sake, restraints were labeled R1, R2, R3, and R4 in order from the side of the rupture disk. The strain gages attached to the clevises of restraint were utilized in order to measure the restraint reaction force, but in RUN 5407, the exact restraint force could not be obtained because of the standard type of clevis. So in RUN 5501, RUN 5603 and RUN 5504, the new type of clevis was designed in order to be able to measure the restraint force exactly. The configuration of this new type of clevis is shown in Fig.2.4.

The amplified outputs from these devices were recorded in the analog data recorder. The response frequency of the total data recorder system was

over 20 kHz. The initial point of recording was the time when the electric current initiates to charge in the arc electrode. The arc current started just after the time when the data recorder and high speed camera attained a steady state.

Two high speed cameras were used. One was for the overall view and another was for the view near restraints. A steam shielding plate was used for protecting the camera from steam. Photographic conditions of the high speed camera are shown in Table 2.4.

The location of scribing points for measuring residual strains on the pipe and restraints is shown in Fig.2.9. The variations of the outer diameters of the test pipe were also measured at these points in order to know the ovallization of the pipe. Measurements were done before and after the tests.

Measuring points for residual displacement of the test pipe are shown in Fig.2.10. The height of marking points from the test bed was measured by a transit before and after the test.

In RUN 5603, equipment for tracing the pipe movement was used as shown in Fig.2.11. The needles of the pen welded to the test pipe scratched the surface on the tracing plate along with the pipe movement. This equipment enabled us to know the deformation of the test pipe when the pipe movement attained to the maximum. Photo 2.2 shows a test pipe and restraints before the test in RUN 5603, and Photo 2.3 shows the view of the test system.

Table 2.1 Chemical Composition and Mechanical Properties

(a) Test Pipe (Room Temperature)

C	Si	Mn	P	S	Ni	Cr
0.5	0.47	1.43	0.026	0.03	9.20	18.35

Yield Strength	Tensile Strength	Elongation
24.8	61.4	56.8

(b) Restraint (Room Temperature)

C	Si	Mn	P	S	Cr	Ni
0.05	0.56	1.57	0.027	0.005	18.33	9.51

Yield Strength	Tensile Strength	Elongation
33.4	61.9	64.9

Table 2.2 Test Condition

Run Number		5501	5407	5603	5504	
Pressure (MPa)		6.8	6.7	6.8	6.9	
Temperature (°C)	Vessel	285	283	284	287	
	Test Section	281	282	281	282	
Diameter and Thickness of Test Pipe		4B, sch 80				
Length of Test Section		3000 mm				
Restraint	Type	U-bar				
	Overhang (mm)	250	400	550	1000	
	Clearance (mm)	100				
	Diameter (mm)	8				
	Number	4				

Table 2.3.1 List of Measurering Items in RUN 5501

TAG No.	LOCATION	SPECIFICATION	MANUFACTURER TYPE	RECORD DEVICE
XU 111 ↑ ↓ XU 127	PIPE SEE Fig.2.7.1	HIGH TEMP SPOT WELDED PLASTIC STRAIN GAGE	AILTECH SG-125-01F-10	L L L M ↑ ↓ M
WU 130 WU 131	RESTRAINT No. 1 SEE Fig.2.8.1	ELASTIC STRAIN GAGE	KYOWA KFD-2-D16-11	M ↑ ↓ M
XU 132 ↑ ↓ XU 139		PLASTIC STRAIN GAGE	TOKYO SOKKI YL-5	L ↑ ↓ L
XU 129		ELASTIC		
WU 140 WU 141	RESTRAINT No. 2 SEE Fig.2.8.1	ELASTIC STRAIN GAGE	KYOWA KFD-2-D16-11	M ↑
XU 142 ↑ ↓ XU 149		PLASTIC STRAIN GAGE	TOKYO SOKKI YL-5	↓ M L
WU 150 WU 151	RESTRAINT No. 3 SEE Fig.2.8.1	ELASTIC STRAIN GAGE	KYOWA KFD-2-D16-11	M ↑
XU 152 ↑ ↓ XU 159		PLASTIC STRAIN GAGE	TOKYO SOKKI YL-5	↓ M L

Table 2.3.2 List of Measurering Items in RUN 5501

TAG No.	LOCATION	SPECIFICATION	MANUFACTURER TYPE	RECORD DEVICE	
WU 160 WU 161 XU 164 XU 169	RESTRAINT No. 4 SEE Fig.2.8.1	ELASTIC STRAIN GAGE	KYOWA KFD-2-D16-11		M M L
		PLASTIC STRAIN GAGE	TOKYO SOKKI YL-5		
PU 101 103 105	SEE Fig.2.6	PRESSURE STRAIN GAGE TYPE	BLH GP-H	ON	H H
110 111 112	SEE Fig.2.7.1		KYOWA PE200KJ		
TU 101 102 104	SEE Fig.2.6	TEMPERATURE C-A SHEATH TYPE	OKAZAKI T-35	ON ON	
130 131 132	SEE Fig.2.7.1		SUKEGAWA		
WU 101 WU 111	SEE Fig.2.6	LOAD CELL STRAIN GAGE TYPE	BLH T2G-1 KYOWA LC5TFH	ON	
XU 200 XU 201	SEE Fig.2.7.1	DISPLACEMENT EDDY CURRENT	SHIN NIPPON SOKKI NP-1000 (503-F)		
XU 300 301 302	SEE Fig.2.7.1	ACCELERATION PIEZO ELECTRIC	SHIN NIPPON SOKKI 541-ASH		
WU 115	SEE Fig.2.6	WATER LEVEL	FUJI FEC-3-4-N3-1		

Table 2.4 High Speed Camera Conditions

	5603		5504	
View	Whole	Restraint	Whole	Restraint
Speed (Frame/sec)	3000	3000	3000	3000
Lens	6.5 m/m	57 m/m	15 m/m	50 m/m
Distance	3.1 m	3.3 m	3.0 m	3.0 m
Iris	F2.8	F2.5	F2.8	F4.0

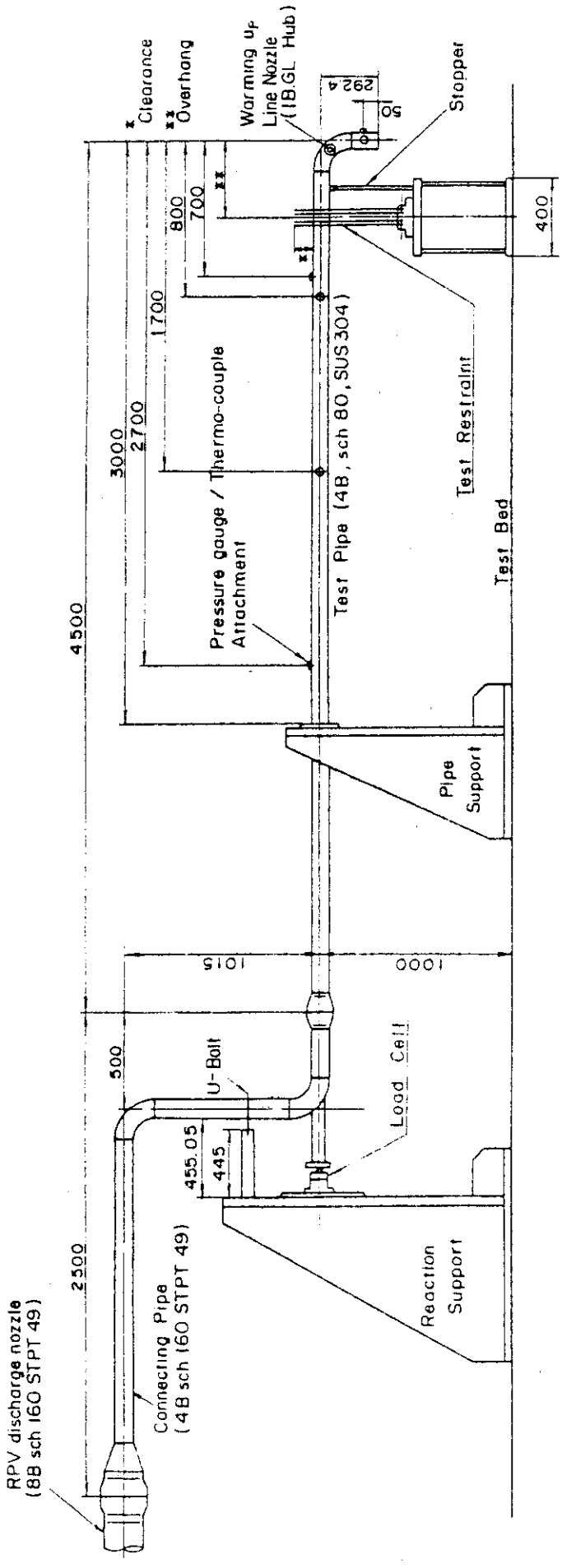

Fig. 2.1 Arrangement of Test Section

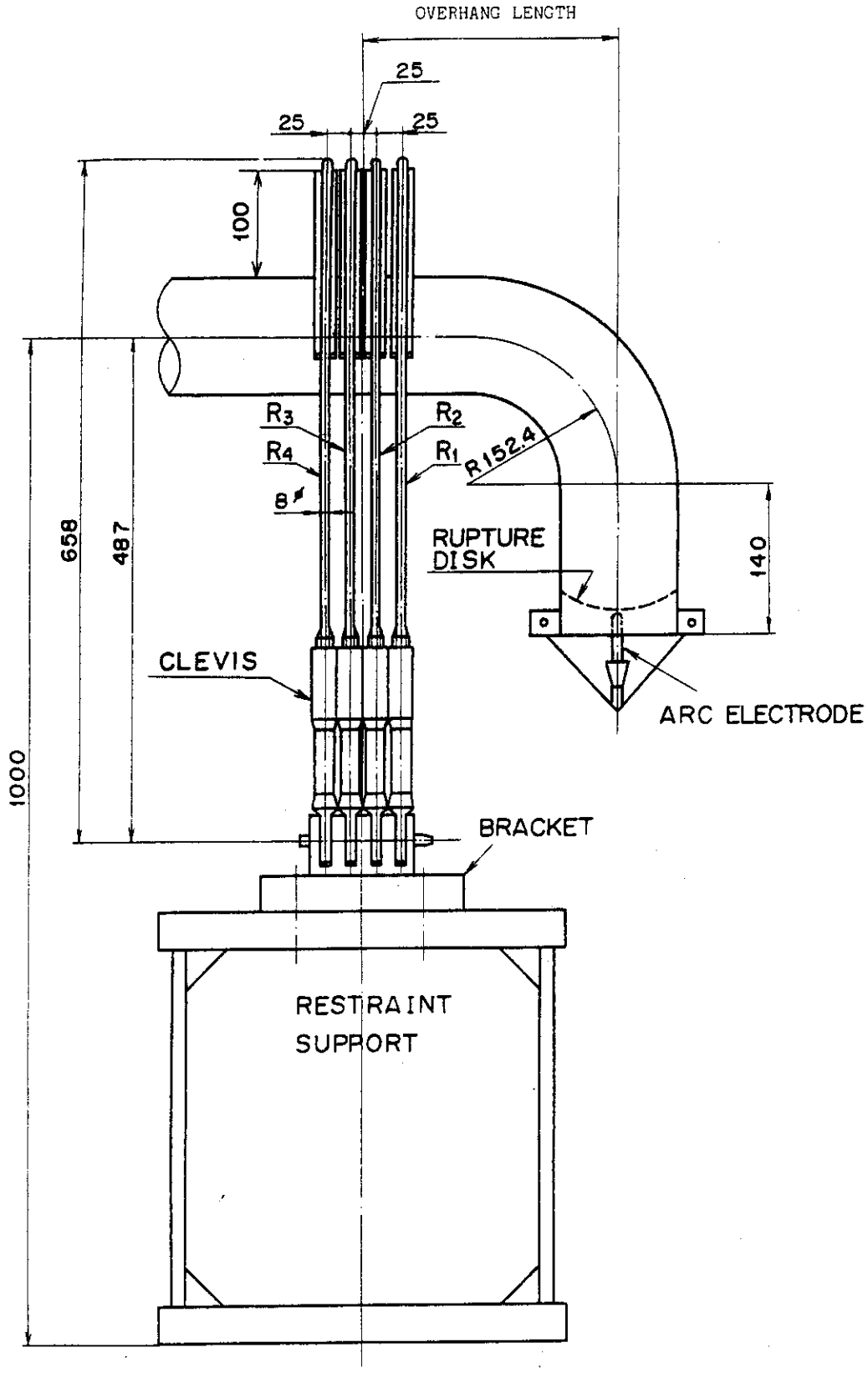

Fig.2.2 Details of Test Pipe

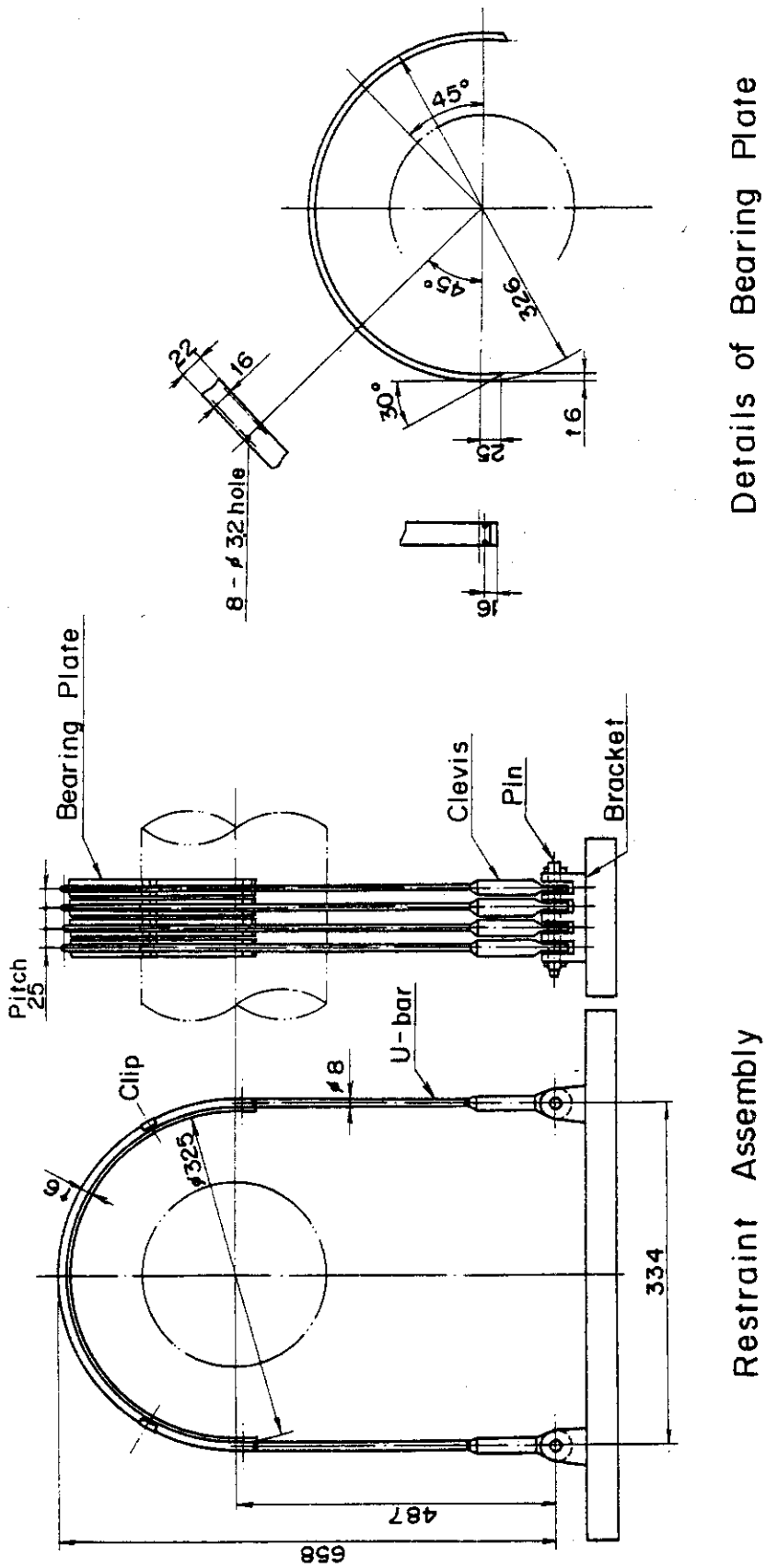

Restraint Assembly

Details of Bearing Plate

Fig.2.3 Restraint Configuration

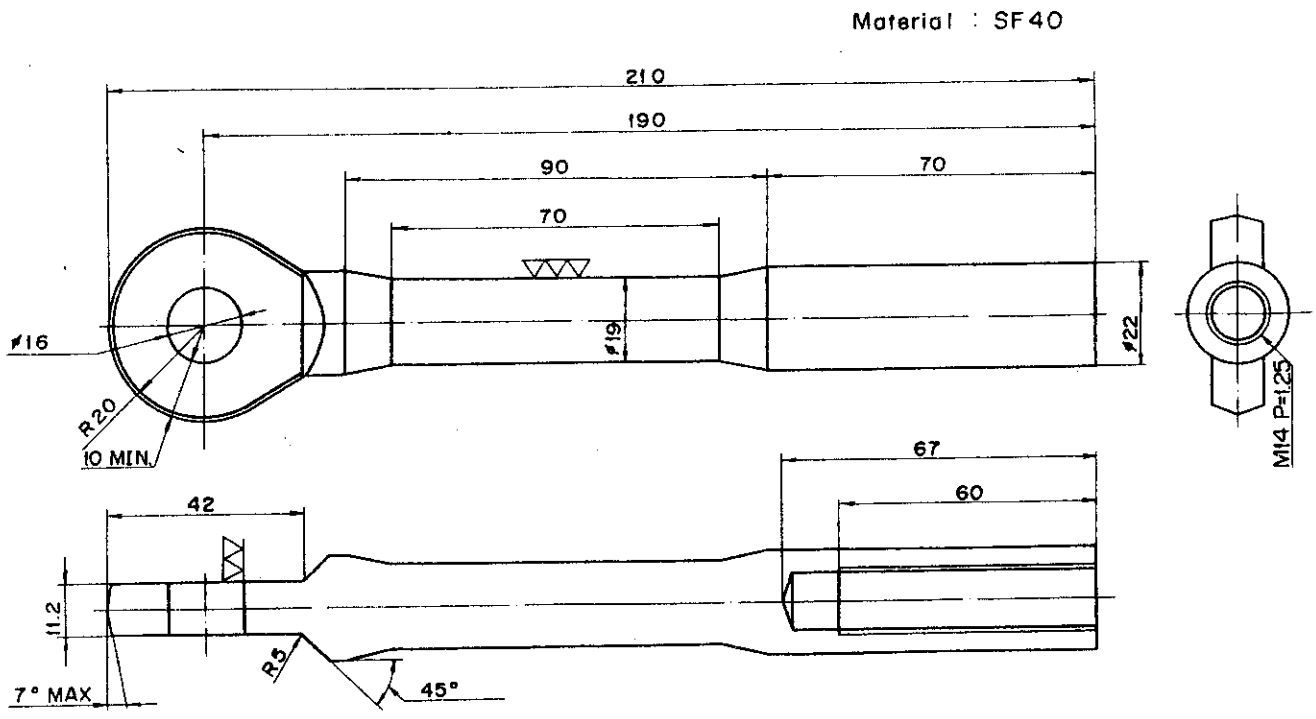

Fig.2.4 Details of Clevis

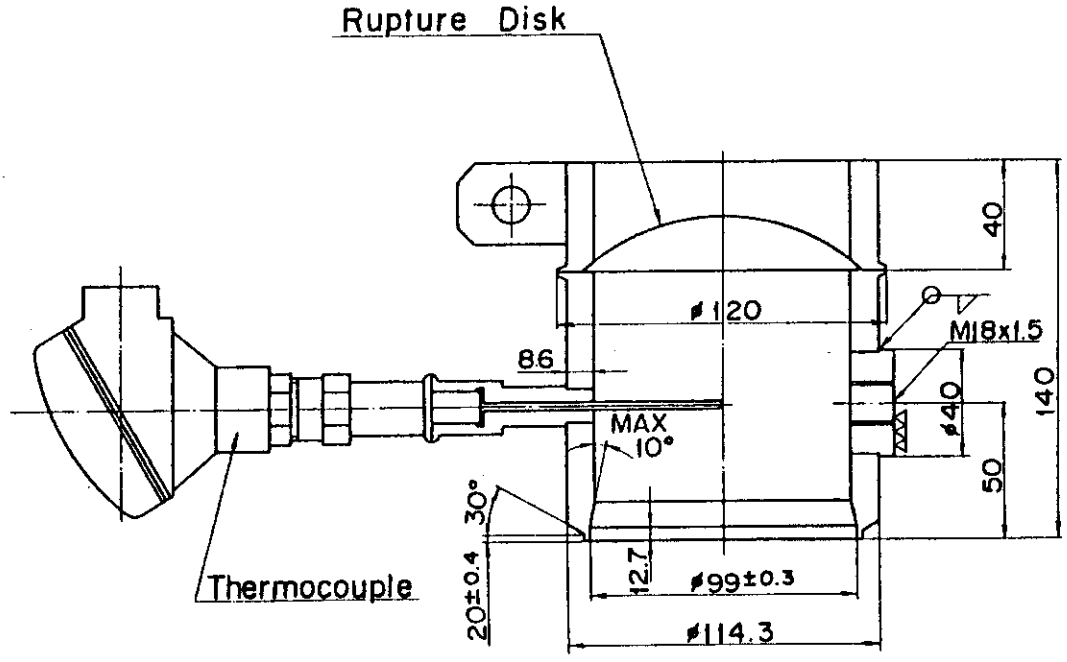

Fig.2.5 Details of Welded Rupture Disk

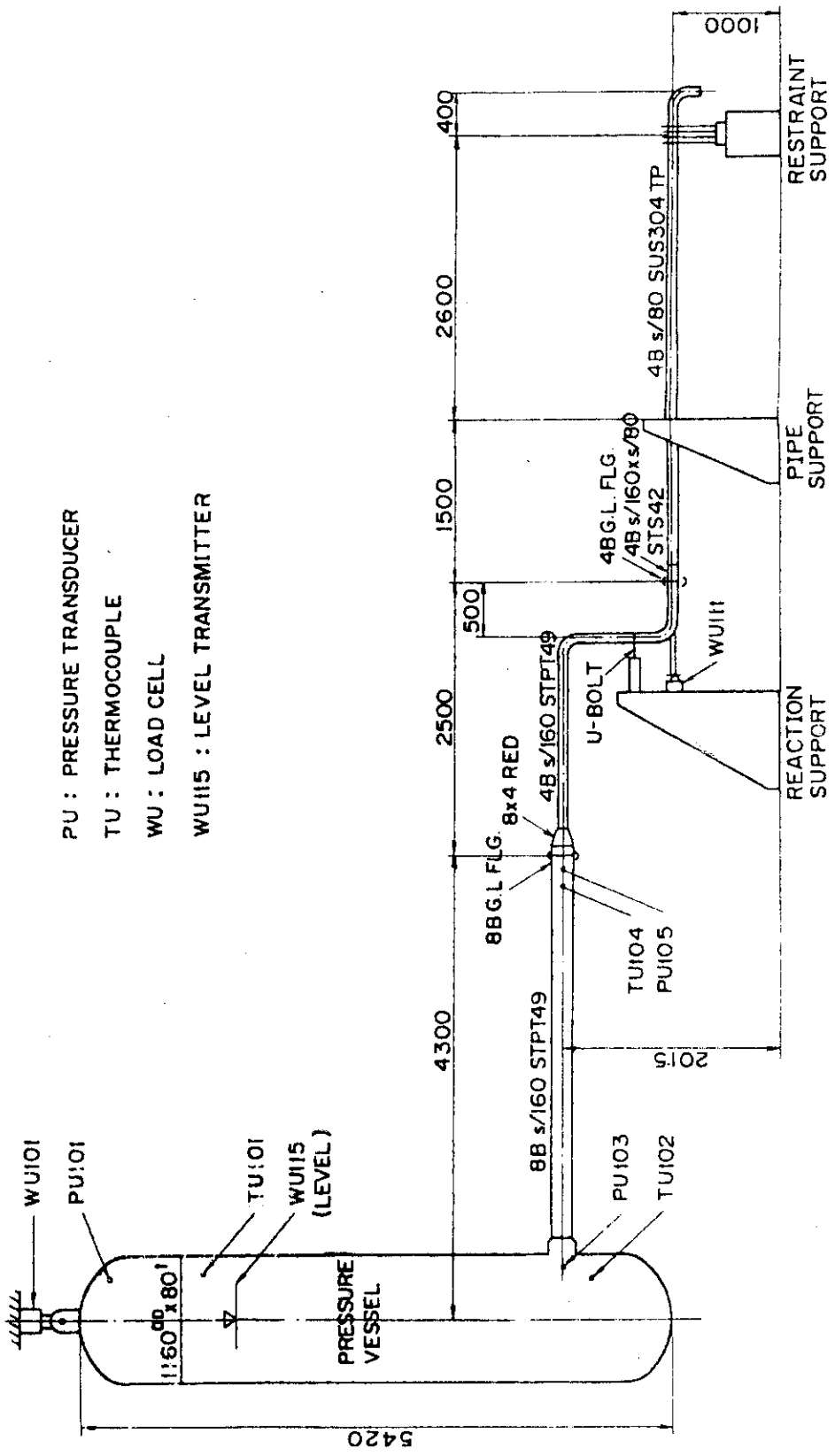

Fig.2.6 Pipe Line Layout of Pipe Whip Test

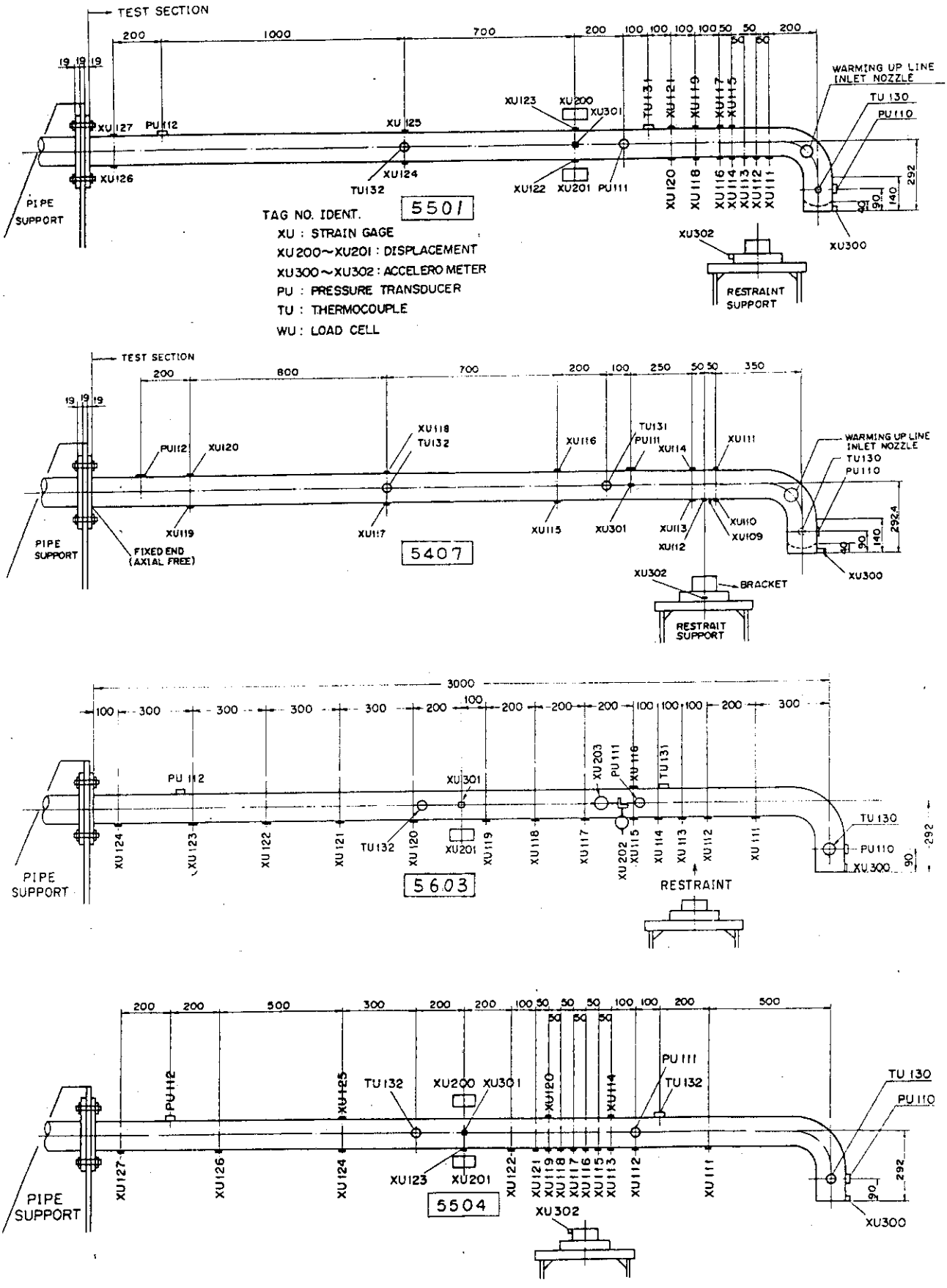

Fig.2.7 Locations of Test Detectors

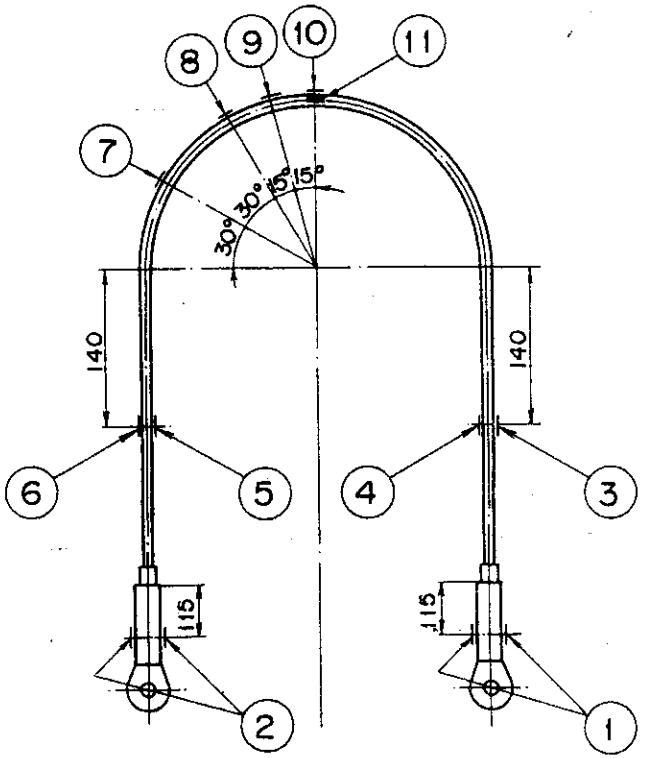

Location	Tag Number			
	Restraint 1	Restraint 2	Restraint 3	Restraint 4
①	WU 130	WU 140	WU 150	WU 160
②	WU 131	WU 141	WU 151	WU 161
③	X U 132	X U 142	X U 152	
④	X U 133	X U 143	X U 153	
⑤	X U 134	X U 144	X U 154	X U 164
⑥	X U 135	X U 145	X U 155	X U 165
⑦	X U 136	X U 146	X U 156	
⑧	X U 137			
⑨	X U 138			
⑩	X U 139	X U 149	X U 159	X U 169
⑪	X U 129			

Fig.2.8.1 Location of Strain Gages in RUN 5501

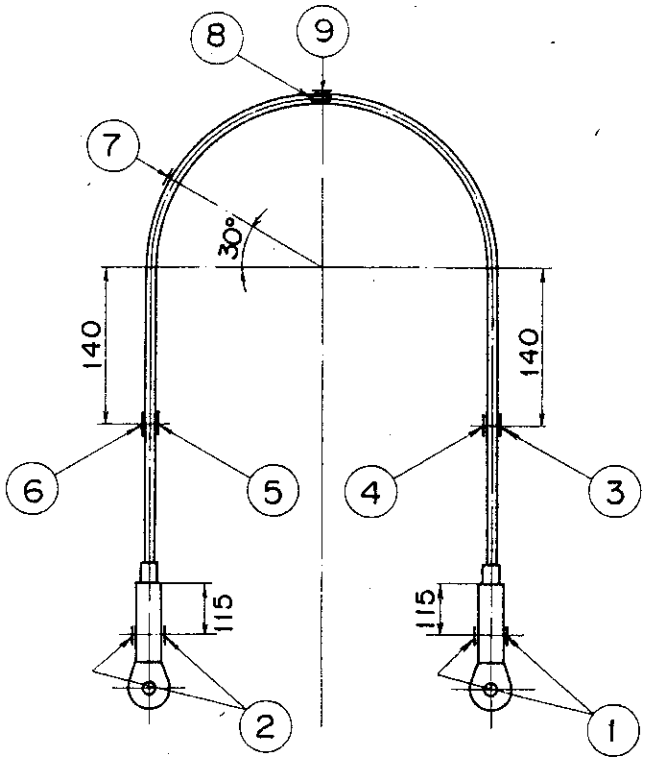

Location	Tag Number			
	Restraint 1	Restraint 2	Restraint 3	Restraint 4
①	WU 130	WU 140	WU 150	WU 160
②	WU 131	WU 141	WU 151	WU 161
③	X U 132	X U 142	X U 152	
④	X U 133	X U 143	X U 153	
⑤	X U 134	X U 144	X U 154	X U 164
⑥	X U 135	X U 145	X U 155	X U 165
⑦	X U 136	X U 146	X U 146	
⑧	X U 138	X U 148	X U 158	
⑨	X U 139	X U 149	X U 159	X U 169

Fig.2.8.2 Location of Strain Gages in RUN 5504

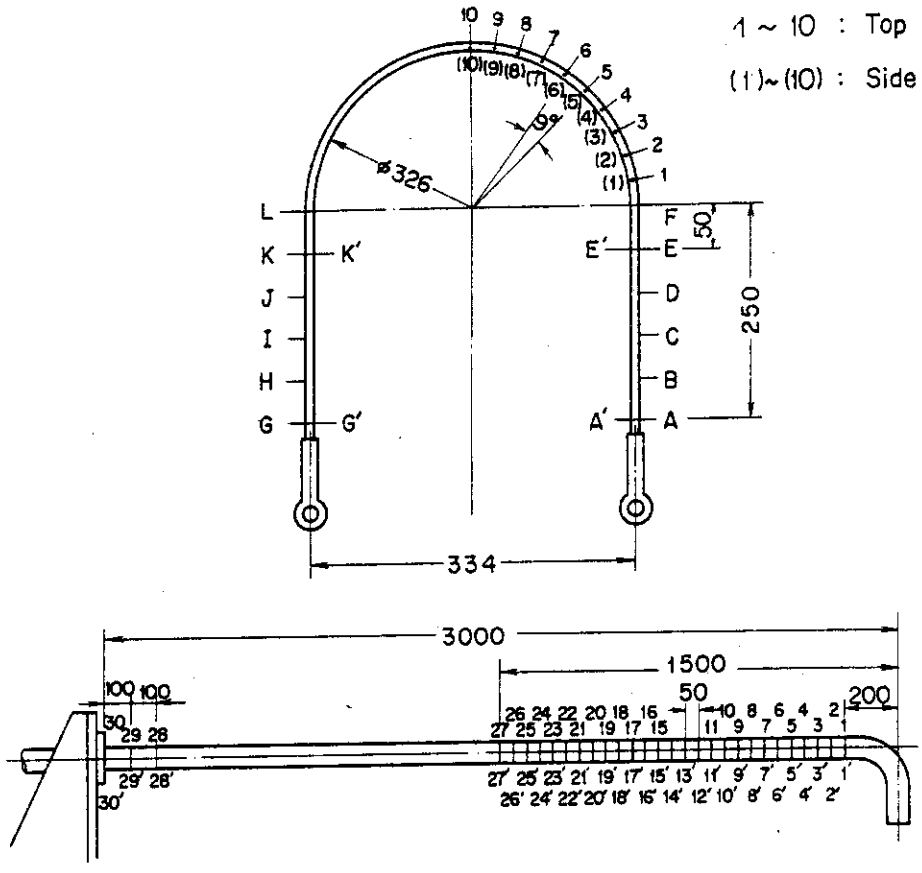

Fig.2.9 Location of Scribing Points

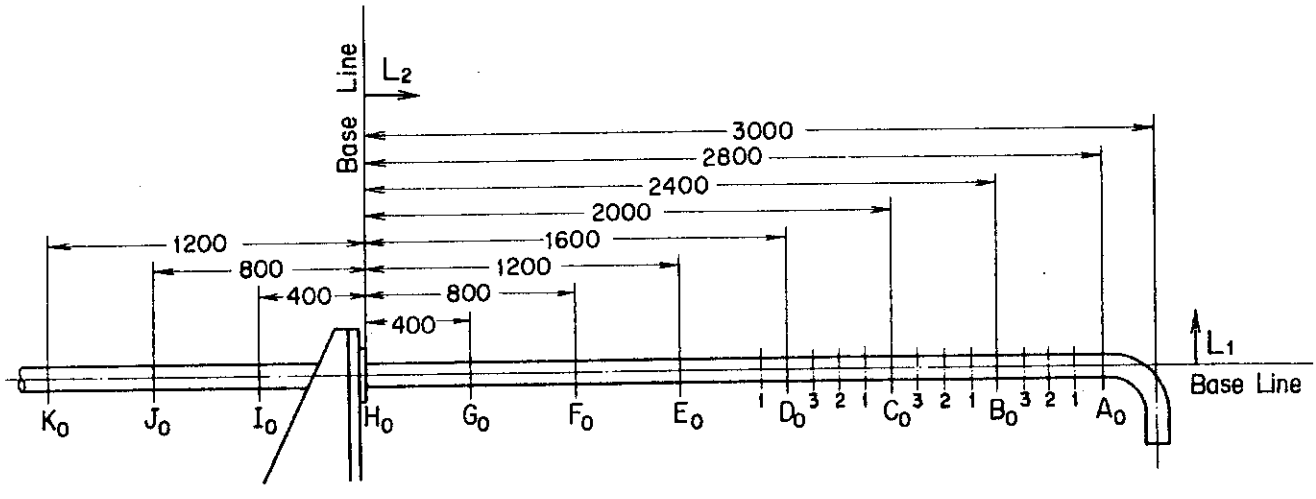

Fig.2.10 Measuring Points of Pipe Displacement

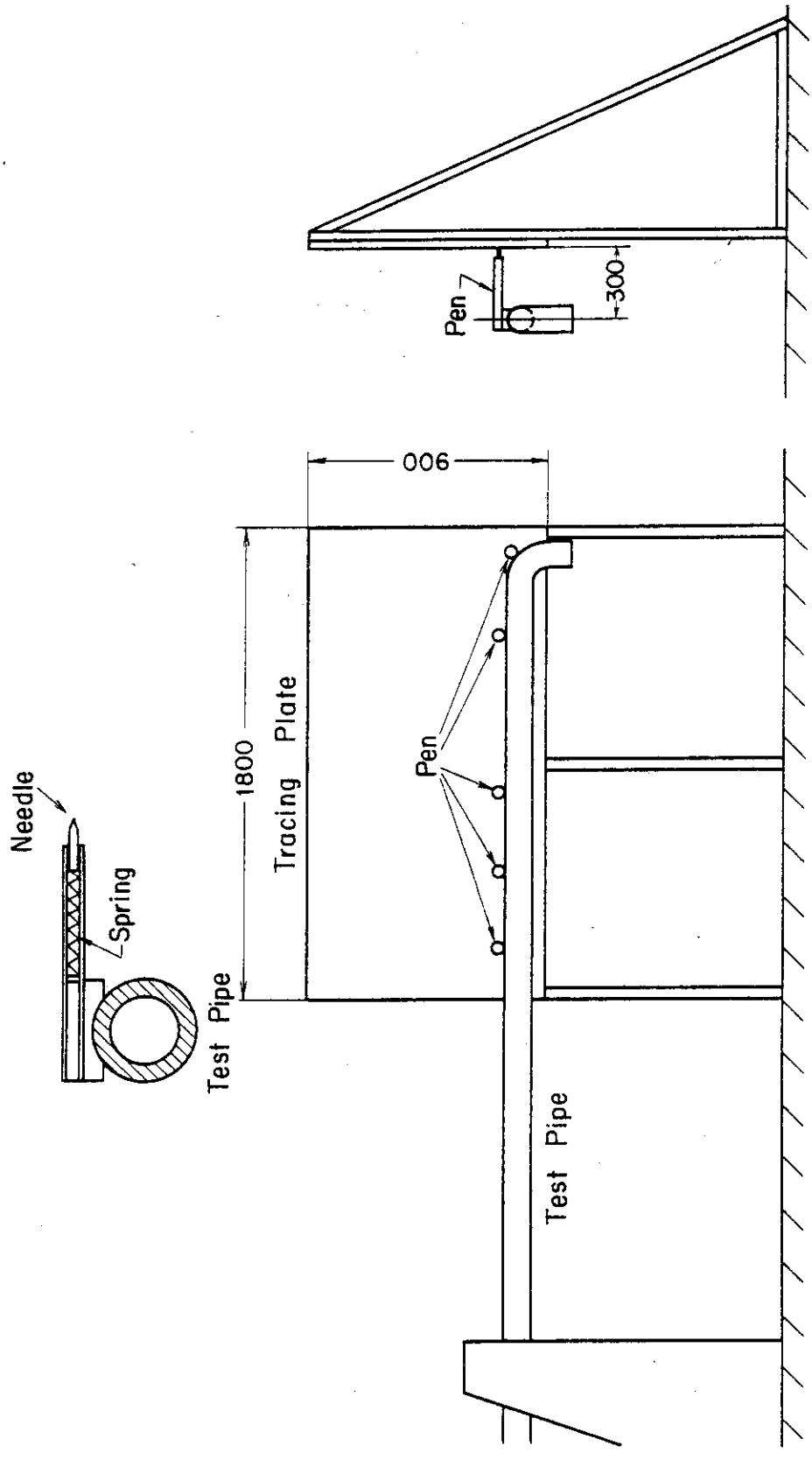

Fig.2.11 Equipment for tracing of pipe movement

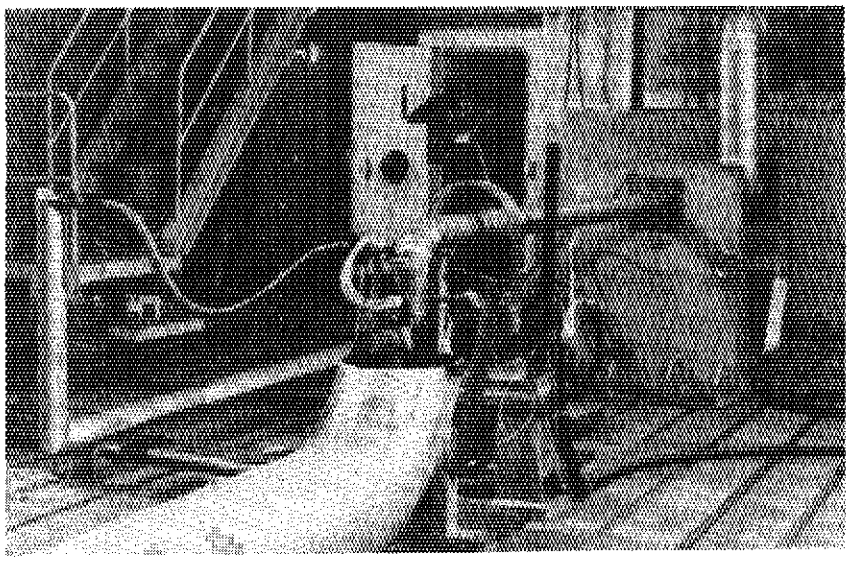

Photo. 2.1 View of the Test System

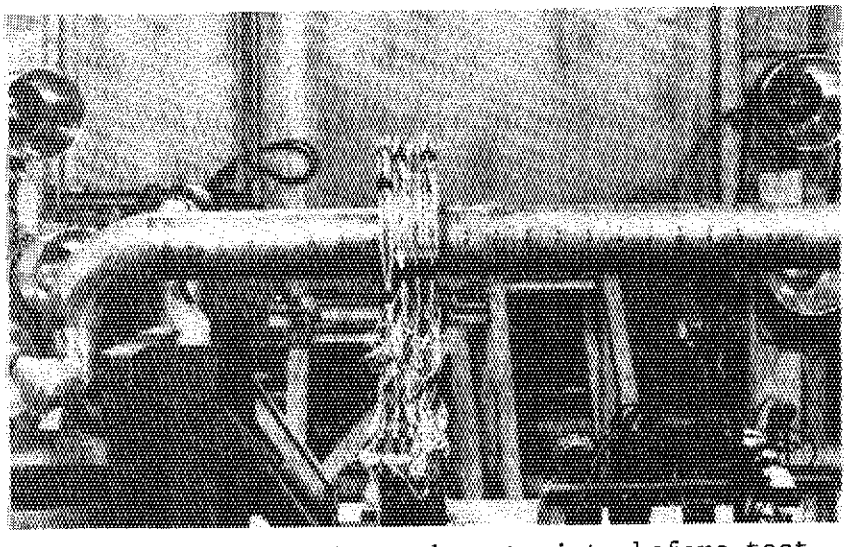

Photo. 2.2 Test pipe and restraints before test

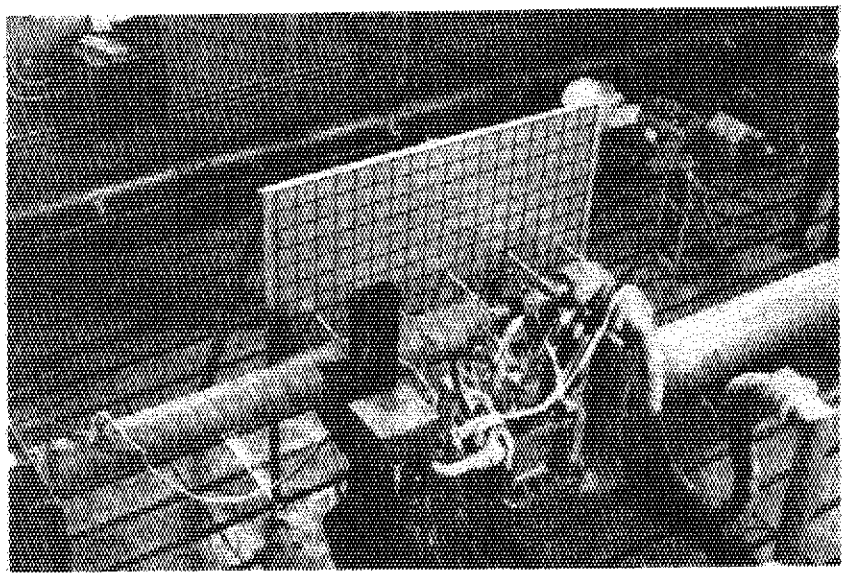

Photo. 2.3 Set up view of the test system

3. TEST RESULTS

3.1 Pressure and Temperature

Output signals from each detector were recorded into an analog tape temporarily, thereafter their time histories were drawn across the paper of the X-Y plotter through the data recorder system and the mini-computer. A code generating system made it possible to search the tape automatically and initializing the time axis. Starting point, Time=0, in the output-time histories does not mean the moving instant of the test pipe but the instant when the electrode discharged sparks.

The initial conditions of pressure and temperature have already been shown in Table 2.2. Pressure-time histories (PU 101) in the pressure vessel are shown in Fig.3.1. Both pressures in RUN 5501 and RUN 5407 have almost the same curves and drop about 0.3 MPa during 5.0 sec after breaking and thereafter reduce slowly. The knee where the discharging jet changes from hot water into steam one appears 18 sec after breaking. Thereafter pressure drops rapidly and the total blowdown time is over 70 sec. The pressure in RUN 5504 scarcely changes during 70 sec, because the pipe collapsed at the restraint point and the fluid was choked up as shown in the preceding section 3.4.

Temperature-time histories (TU101) of the fluid temperature in the pressure vessel are shown in Fig.3.2. Both fluid temperatures in RUN 5501 and RUN 5407 have almost the same curves and these temperatures correspond to the pressures curve from 2 sec to 60 sec. After 60 sec, temperature rises rapidly because of heating from the vessel wall. The fluid temperature in RUN 5504 scarcely changes during 70 sec because of the choking due to the collapsed pipe.

The representative pressure-time histories (PU 110, PU 111) in the

test pipe are shown in Fig.3.3. In RUN 5501 and RUN 5407, pressures drop in stepwise manner just after breaking and thereafter hardly change and drop about 35 kg/cm^2 in the range of 0.7 sec. In RUN 5504, pressure in the test pipe reduces to 0.0 kg/cm^2 because of the choking due to the collapsed pipe.

3.2 Strain-Time History

Typical time histories of pipe strain are shown in Fig.3.4. These measuring points are at the outer surface of the pipe under the restraint. The strain in RUN 5501 is smaller than others, but the strain in RUN 5504 is not measured because of the large deformation of the test pipe. It is understood that the generation of a plastic hinge at restraints is affected by the overhang length.

Other typical time histories of pipe strain near the pipe support are shown in Fig.3.5. About 40 Hz vibration is included in the output history in RUN 5501. This seems to be the natural frequency of the test pipe between the supporting point and the restraint point. In RUN 5504, the strain gage is snapped because of the large deformation of the pipe near the pipe support.

Typical time histories of strain on restraints are shown in Fig.3.6. These measuring points are the straight portion of restraint R1. In RUN 5504, the steady strain after the first peak is meaningless data, because four restraints are folded by the test pipe. Steady state values and peak values of strain gages attached on restraints are summarized in Table 3.1.

Averaged peak strains at the straight portion of restraint are shown in Fig.3.7. The peak strain in RUN 5407 is the highest of the four cases.

This depends on the relation between the effective mass and the deformation of the pipe. That is, the effective mass of a pipe acting on the restraint in RUN 5407 is larger than that in RUN 5501 because of the difference of overhang length. The energy up to impact is proportional to the effective mass of pipe and the peak strain of the restraint increases. On the other hand, in RUN 5504, the effective mass of pipe increases but the peak strain of the restraint does not increase so much since the energy is dissipated in the deformation of the test pipe.

Restraint reaction forces in RUN 5501 are shown in Fig.3.8.1 and Fig.3.8.2. These forces were converted from strain gages attached to the clevises of restraint. Restraint reaction forces were measured from eight clevises. It seems that these restraints rebound a few times after impact with the test pipe. The steady force of restraint R1 is the highest of the four restraints, but the steady force of restraint R4 is almost zero. This means that the four restraints act in effect instantaneously after the impact, but restraints such as R3, R4 separate from the pipe in the steady state.

A detailed force-time history of restraint R1 is shown in Fig.3.9. A small peak at about 32 msec indicates the instant of impact between the pipe and restraints. Maximum force is about 2.1 ton (20.6 kN) at about 38 msec. After that time, this force reduces rapidly to zero. This means that the pipe separates from the restraint instanteneously after impact. It is apparent from this figure that the period of this rebound phenomenon is about 6 msec. Steady and peak values of the restraint reaction forces are summarized in Table 3.2.

The time sequence of major events is shown in Fig.3.10. Time=0 is the start of data recording. XU 300 is an accelometer attached to a free pipe end. The starting time of the output of XU 300 means the moving instant

of the test pipe. XU 139 is the strain gage attached to the top of restraint R1. XU 169 is the strain gage attached to the top of restraint R4. The starting time of these outputs means the instant of impact between a pipe and a restraint. Impact time which is the elapsed time from the rising time of the accelometer XU 300 to that of the strain gage XU 139 is also shown in Fig.3.10.

3.3 High Speed Camera Photography

Photographs taken by high speed cameras in RUN 5603 and RUN 5504 are shown in Photo 3.1 and Photo 3.2 respectively. The overall views and the local views near restraints are included in these photographs. Photographs in RUN 5501 could not be obtained because the film was cut just after the starting of high speed camera. Frames start just after the blow-down and the interval is 3.33 msec.

Restraints slided along the pipe axis after the impact between the pipe and restraints, and it seemed to increase the overhang length. They, the free pipe end moved upwards and tore off the warming up line. At last the pipe collapsed and folded in two.

Angular velocity for a free pipe end is calculated from these photographs and is summerized in Table 3.3. At first, angular velocity was slow because of the gradual acceleration from a stationary state into a dynamic one. After the generation of the plastic hinge, the angular velocity further increased.

3.4 Residual Deformation

Static strains of various kinds of detectors before and after the test RUN 5501 are summarized in Table 3.4.1 to Table 3.4.3. Residual strains of the pipe are smaller than those of restraints. Residual strains of the pipe in RUN 5501 are summarized in Table 3.5. The axial distribution of residual pipe strains in RUN 5501 is shown in Fig.3.11. These residual strains were calculated from the distances of marks before and after the test. Black points are residual strains obtained from strain gages attached to a pipe. Residual strain in RUN 5501 is small because of a short overhang length, 250 mm.

Residual strains of the pipe in RUN 5504 are summarized in Table 3.6. This distribution along the pipe axis is shown in Fig.3.12. Maximum residual strain in RUN 5504 is about 22% at the position of 1200 mm from the free pipe end. A plastic hinge is generated at a position nearby the setting point of restraints because of sliding of the U-bars along the pipe axis.

Results of dimensional measurements in RUN 5501 are summarized in Table 3.7. The distribution of residual strain of the restraint is shown in Fig.3.13. This is the comparison between RUN 5501 and RUN 5407. These residual strains were measured from the points marked on a restraint R1. Residual strain in RUN 5501 is generally less than that in RUN 5407, because the effective mass of the pipe at the instant of impact in RUN 5501 is less than that in RUN 5407. The effective mass means the mass between the free end of pipe and the setting point of restraint. It seems that four restraints act uniformly because of the small deformation of the pipe in RUN 5501.

Fig.3.14 shows the distribution of residual strain of the four restraints in RUN 5603, OH = 550 mm. The first restraint R1 deforms the most of the four restraints because of the long overhang length. That is, when the

overhang length is long, the test pipe bends steeply at the setting point of restraints as shown in Photo.3.1, and hence the restraint R1 gives the highest resistance to the test pipe and deforms the most of the four restraints. Deformed restraints in RUN 5501, RUN 5603 and RUN 5504 are shown in Photo.3.2, Photo.3.3 and Photo.3.4.

Displacements of the pipe in RUN 5501 are summarized in Table 3.8. The distribution of residual deformation along the pipe axis is shown in Fig.3.15, which is the comparison between RUN 5501 and RUN 5407. These deformations were measured by a transit after tests. The deformation in RUN 5407 is more violent than that in RUN 5501 at the free pipe end. This relates to the fact that the bending moment in RUN 5407 is larger than that in RUN 5501 because of the difference of overhang lengths. The situation of this pipe before and after the test is shown in Photo.3.5.1 and Photo.3.5.2.

Fig.3.16 shows the difference between the residual deformation and the maximum deformation of the test pipe in RUN 5603, OH = 550 mm. The maximum deformation of the test pipe was measured by the scratching line on the surface of the tracing plate as shown in Photo.3.6.3. View of the test system after the test RUN 5603 is shown in Photo.3.6.1, and the situation of the pipe and restraints after the test is shown in Photo.3.6.2. Photo.3.6.4 shows a rupture disc after the test.

In RUN 5504, a pipe was folded in two around the setting point of restrants because of too long overhang length. Residual deformation of the pipe measured after the test is shown in Fig.3.17. Situations of this pipe before and after the test are shown in Photo.3.7.1 and Photo.3.7.2.

Results of measuring diameters of the pipe before and after the test in RUN 5501 are summarized in Table 3.9. These variations along the pipe axis are shown in Fig.3.18. Vertical diameters expand and horizontal

diameters decrease in spite of vertical impact between the pipe and restraints, but these differences are negligible, so the pipe does not crash plastically in RUN 5501.

Results of measuring diameters of the pipe before and after the test in RUN 5504 are summarized in Table 3.10. These variations along the pipe axis are shown in Fig.3.19. Horizontal diameters expand about 40 mm at the position of 1200 mm from the free pipe end.

Table 3.1 Steady State Values and Peak Values of Strain Gages

(%)

		RUN 5501, OH = 250				RUN 5603, OH = 550				RUN 5504, OH=1000			
		R1	R2	R3	R4	R1	R2	R3	R4	R1	R2	R3	R4
XU1-2	Steady	0.60	0.35	0.10	—	0.90	0.20	0.15	-0.09	—	—	—	—
	Peak	0.50	0.45	0.25	—	1.50	0.30	0.20	-0.14	0.60	1.10	0.20	—
XU1-3	Steady	0.60	0.25	0.10	—	1.90	0.25	0.20	0.13	—	—	—	—
	Peak	0.60	0.45	0.30	—	1.50	0.40	0.33	0.35	0.70	0.35	0.15	—
XU1-4	Steady	0.65	0.30	0.15	0.10	2.60	0.35	0.17	-0.10	—	—	—	—
	Peak	0.70	0.45	0.30	0.25	1.70	0.50	0.27	-0.13	0.85	0.35	0.15	0.00
XU1-5	Steady	0.95	0.15	0.05	0.00	—	0.25	0.18	0.18	—	—	—	—
	Peak	1.20	0.30	0.20	0.20	—	0.40	0.24	0.41	1.60	0.30	0.20	0.20
Ave.	Steady	0.70	0.26	0.10	0.05	1.80	0.26	0.18	0.03	—	—	—	—
	Peak	0.75	0.41	0.26	0.23	1.57	0.40	0.26	0.12	0.94	0.53	0.18	0.10

Note: Data for RUN 5407 were summarized in Table 3.5 of JAERI-M 9496.

Table 3.2 Restraint Force

ton (kN)

	RUN 5501 (OH=250)		RUN 5603 (OH=550)		RUN 5504(OH=1000)	
	Steady	Peak	Steady	Peak	Steady	Peak
WU 130	1.0 (9.8)	2.2 (21.6)	1.5(14.7)	2.3 (22.5)	—	2.1(20.6)
WU 131	1.2(11.8)	2.2 (21.6)	1.6(15.7)	2.3 (22.5)	—	1.9(18.6)
WU 140	0.7 (6.9)	2.1 (20.6)	-0.1(-1.0)	2.1 (20.6)	—	1.8(17.6)
WU 141	0.6 (5.9)	2.1 (20.6)	0.2 (2.0)	2.1 (20.6)	—	1.8(17.6)
WU 150	0.1 (0.9)	1.7 (16.7)	0.5 (4.9)	1.6 (15.7)	—	0.6 (5.9)
WU 151	0.2 (1.8)	1.8 (17.6)	0.5 (4.9)	1.5 (14.7)	—	0.6 (5.9)
WU 160	0.1 (0.9)	1.2 (11.8)	-0.1(-1.0)	1.0 (9.8)	—	0.4 (3.9)
WU 161	0.2 (1.8)	1.2 (11.8)	0.0 (0.0)	0.9 (8.8)	—	0.4 (3.9)
Total	4.1(40.2)	14.5(142.1)	4.1(40.2)	13.8(135.2)	—	9.6(94.1)

Note 1. Steady force is that 0.5 sec after rupturing.

2. Peak force is that of the first peak.

3. DLF is determined by deviding the restraint force by the thrust force, T_p = 2.64 ton (25.9 kN)

Table 3.3 Angular Velocity of Whipping Pipe at Each Elapsed Time

Time	Angular Velocity
t (m sec)	θ (rad/sec)
0.0 ∿ 20.0	8.81
20.0 ∿ 30.0	17.63
30.0 ∿ 40.0	"
40.0 ∿ 50.0	"
50.0 ∿ 60.0	"
60.0 ∿ 65.0	35.25
65.0 ∿ 70.0	"
70.0 ∿ 75.0	"
75.0 ∿ 80.0	"

Note: 1. Time means the elapsed time from ruptured instant.

2. Angular velocity is averaged between two elapsed times.

Table 3.4.1 Static Strains Before and After Test in RUN 5501

TAG No.	BEFORE ①	AFTER ②	②−①
XU 111	11,265	12,515	1,250
112	9,421	11,607	2,186
113	10,965	12,895	1,930
114	10,632	11,901	1,269
115	10,524		
116	9,490	10,269	779
117	10,675	9,730	−945
118	10,045	11,817	772
119	9,255	8,231	−1,024
120	13,065	14,457	392
121	12,955	10,315	−2,640
122	10,466	12,136	1,670
123	12,219	10,403	−1,816
124	9,385	9,756	371
125	10,958	10,863	−95
126	11,320	13,441	2,121
127	9,382	8,295	−1,087
WU 130	10,205	10,245	40
131	8,580	8,632	52
XU 132	11,670	16,315	4,645
133	13,260	18,460	5,200

(μ)

Table 3.4.2 Static Strains Before and After Test in RUN 5501

TAG No.	BEFORE ①	AFTER ②	②−①
XU 134	13,005	18,296	5,291
135	13,224	17,290	4,066
136	13,596	7,990	−5,606
137	13,521	20,107	6,586
138	11,957		
139	12,035		
129	10,897	18,257	7,360
WU 140	8,618	8,710	92
141	10,717	10,732	15
XU 142	11,125	12,582	1,457
143	12,166	14,603	2,437
144	10,667	12,698	2,031
145	13,287	14,460	1,173
146	13,885	6,905	−6,980
149	12,136		
WU 150	11,146	11,199	53
151	10,541	10,592	51
XU 152	11,173	11,560	387
153	12,590	13,846	1,274
154	12,745	14,171	1,426
155	13,765	14,192	427

(μ)

Table 3.4.3 Static Strains Before and After Test in RUN 5501

TAG No.	BEFORE ①	AFTER ②	②−①
XU 156	12,960	2,325	−10,635
159	12,266		
WU 160	8,998	9,090	92
161	9,073	9,141	98
XU 164	12,786	13,522	1,087
165	12,435	12,302	−133
169	13,011		
PU 101	11,055	11,047	−8
103	11,103	11,170	67
105	11,045	11,040	−5
110	11,161	10,522	−639
111	11,152	10,505	−647
112	11,066	10,475	−591
WU 110	13,662	13,606	−54
111	11,020	11,154	−134

(μ)

Table 3.5 Residual Strains of Pipe in RUN 5501

	Compression Side			Tension Side		
	L_1	L_2	ε	L_1'	L_2'	ε'
1 – 2	50.00	49.90	−0.20	50.35	50.30	−0.10
2 – 3	49.90	49.80	−0.20	50.40	50.45	0.10
3 – 4	50.30	50.25	−0.10	50.50	50.65	0.30
4 – 5	49.65	49.55	−0.20	49.55	49.70	0.30
5 – 6	50.10	50.10	0.00	49.90	49.95	0.10
6 – 7	49.80	49.80	0.00	49.55	49.60	0.10
7 – 8	50.05	50.00	−0.10	50.00	50.15	0.30
8 – 9	50.00	49.75	−0.50	49.50	49.55	0.10
9 – 10	50.40	50.20	−0.40	49.80	49.90	0.20
10 – 11	} 97.55	} 97.50	−0.05	50.00	50.00	0.00
11 – 12				50.30	50.50	0.40
12 – 13	50.40	50.30	−0.20	48.75	48.85	0.21
13 – 14	50.00	49.90	−0.20	49.00	49.15	0.31
14 – 15	49.65	49.60	−0.10	50.10	50.20	0.20
15 – 16	50.10	50.05	−0.10	50.30	50.55	0.30
16 – 17	49.70	49.40	−0.60	49.55	49.70	0.30
17 – 18	50.00	49.80	−0.40	49.60	49.85	0.50
18 – 19	49.40	49.35	−0.10	50.15	50.35	0.50
19 – 20	49.80	49.75	−0.10	49.50	49.80	0.61
20 – 21	49.80	49.65	−0.30	50.00	50.05	0.10
21 – 22	49.80	49.70	−0.20	49.60	49.75	0.30
22 – 23	50.00	49.85	−0.30	49.90	49.95	0.10
23 – 24	49.85	49.75	−0.20	50.15	50.25	0.20
24 – 25	49.90	49.80	−0.20	49.80	49.80	0.00
25 – 26	50.00	49.90	−0.20	49.80	49.80	0.00
26 – 27	49.60	49.55	−0.10	49.70	49.75	0.10
28 – 29	99.75	99.55	−0.20	99.85	100.05	0.20
29 – 30	100.00	99.70	−0.30	99.55	99.85	0.30

L_1, L_1' : Length Before the Test (mm)

L_2, L_2' : Length After the Test (mm)

ε, ε' : Residual Strain (%)

Table 3.6 Residual Strains of Pipe in RUN 5504

	Compression Side			Tension Side		
	L_1	L_2	ε	L_1'	L_2'	ε'
1- 2	50.00	49.45	-1.1	49.20	49.70	1.02
2- 3	98.40	97.90	-0.51	50.40	50.85	0.89
3- 4				50.35	51.05	1.39
4- 5	49.60	48.85	-1.51	49.70	50.80	2.21
5- 6	50.20	48.85	-2.69	49.40	50.60	2.43
6- 7	49.65	47.75	-3.83	49.95	51.80	3.70
7- 8	49.95	47.95	-4.00	49.80	52.40	5.22
8- 9	49.85	47.35	-5.02	49.50	53.70	8.48
9-10	49.85	46.70	-6.32	49.50	54.75	10.61
10-11	49.80	45.95	-7.73	50.60	57.05	12.75
11-12	49.75			49.70	56.75	14.19
12-13	49.85			49.90	60.66	21.34
13-14	49.80			49.55	59.05	19.17
14-15	49.90			50.00	58.45	16.90
15-16	49.95	45.60	-8.71	50.00	56.35	12.70
16-17	49.90	47.00	-5.81	49.90	54.80	9.82
17-18	50.00	48.10	-3.80	49.70	53.35	7.34
18-19	49.90	47.90	-4.01	49.90	52.10	2.09
19-20	49.90	48.50	-2.81	49.80	51.65	3.71
20-21	49.80	48.65	-2.31	49.90	51.45	3.11
21-22	50.00	49.00	-2.00	49.80	50.60	1.61
22-23	49.90	49.30	-1.20	50.10	50.40	0.60
23-24	49.80	49.40	-0.40	49.70	49.90	0.40
24-25	49.90	49.60	-0.60	49.80	50.15	0.70
25-26	49.95	49.50	-0.90	49.80	50.00	0.40
26-27	49.85	49.50	-0.70	49.80	50.00	0.40
28-29	99.80	104.55	4.76	99.90	96.35	-3.55
29-30	100.20	106.55	6.34	99.80	93.30	-6.51

(μ)

L_1, L_2': Length Before the Test

L_2, L_2': Length After the Test

Table 3.7 Results of Dimensional Measurements in RUN 5501

	5501							
	R1		R2		R3		R4	
A −B	49.80	0.20	49.85	0.15	49.90	0.10	49.90	0.00
B −C	50.10	0.00	49.65	0.05	49.90	0.10	49.80	0.00
C −D	49.80	0.55	50.05	0.10	50.05	0.05	49.85	−0.05
D −E	49.60	0.95	49.80	0.10	49.60	0.05	49.65	−0.05
E −F	50.00	0.45	49.80	0.10	49.65	0.00	49.90	−0.15
A −F	249.90	1.60	249.85	0.45	249.70	0.20	249.75	−0.15
A′−E′	199.95	1.65	200.20	0.50	200.10	0.30	199.85	0.25
G −H	49.70	0.30	49.60	0.10	50.00	0.00	49.75	0.00
H −I	50.00	0.25	50.15	0.05	49.65	−0.10	49.90	0.00
I −J	50.00	0.30	50.05	0.15	50.20	0.10	49.90	0.00
J −K	49.65	0.25	49.50	0.30	49.65	0.00	49.80	0.00
K −L	49.80	0.20	50.00	0.05	50.00	−0.10	49.65	−0.05
G −L	249.90	1.10	250.00	0.50	250.00	0.15	249.60	0.00
G′−K′	199.90	1.00	199.80	0.40	199.70	0.25	199.65	0.10
F − 1	24.75 (24.20)	−0.15 (0.35)	24.80	−0.25	24.80	−0.25	24.80	−0.20
1 − 2	24.90 (24.20)	−0.15 (0.40)	25.00	−0.25	24.85	−0.40	25.00	−0.30
2 − 3	25.10 (24.20)	−0.35 (0.35)	24.80	−0.25	25.00	−0.45	24.85	−0.45
3 − 4	24.70 (24.40)	−0.10 (0.35)	25.00	−0.30	24.90	−0.35	25.10	−0.30
4 − 5	25.05 (24.40)		25.20		24.95		24.00	
5 − 6	24.80 (24.60)		24.95		25.25		25.80	
6 − 7	25.15 (24.50)	0.15 (0.35)	24.85	0.15	24.90	0.10	24.85	0.00
7 − 8	25.10 (24.65)	0.90 (0.65)	25.00	0.85	25.05	0.75	24.90	0.40
8 − 9	25.15 (24.70)	1.40 (0.70)	25.35	1.30	25.00	1.30	25.00	1.00
9 −10	24.80 (24.45)	1.25 (0.35)	24.90	1.10	25.20	0.90	24.95	0.95

LEFT VALUE : ORIGINAL LENGTH (mm)
RITE VALUE : DEVIATION AFTER TEST (mm)

Table 3.8 Displacements of Pipe in RUN 5501

Position		Vertical Disp. L_1	Axial Disp. L_2
A0	2800	117.0	−4.0
A1	2700	110.3	
A2	2600	103.0	
A3	2500	96.2	
B0	2400	89.5	−2.5
B1	2300	82.7	
B2	2200	77.0	
B3	2100	71.5	
C0	2000	66.3	−2.3
C1	1900	61.2	
C2	1800	56.7	
C3	1700	52.5	
D0	1600	48.4	−2.5
D1	1500	44.7	
E0	1200	34.2	−1.7
F0	800	21.0	−1.3
G0	400	9.0	−0.7
H0	0	0.0	0.0

(mm)

Table 3.9 Diameters of Pipe in RUN 5501

	Vertical Dia.			Horizontal Dia.		
L	D_V	D_V'	$D_V' - D_V$	D_H	D_H'	$D_H' - D_H$
2750	114.13	114.23	0.10	114.19	114.14	−0.05
2650	114.20	114.35	0.15	114.13	114.08	−0.05
2550	114.28	114.36	0.08	114.05	114.02	−0.03
2450	114.21	114.27	0.06	113.97	114.00	0.03
2350	113.07	113.28	0.21	114.39	114.71	0.32
2250	113.68	114.02	0.34	113.88	113.74	−0.14
2150	114.72	114.71	−0.01	113.11	113.26	0.15
2050	114.15	114.22	0.07	114.03	114.02	−0.01
1950	114.09	114.25	0.16	114.09	114.03	−0.06
1850	114.14	114.29	0.15	114.02	113.92	−0.10
1750	114.18	114.32	0.14	114.07	113.99	−0.08
1650	114.22	114.27	0.05	114.03	113.95	−0.08
1350	114.15	114.22	0.07	114.16	114.08	−0.08
200	114.12	114.21	0.09	114.14	114.06	−0.08
100	114.20	114.28	0.08	114.17	114.14	−0.03
0	114.10	113.96	−0.14	114.14	114.29	0.15

(mm)

D_V : Vertical Dia. Before the Test

D_V' : Vertical Dia. After the Test

D_H : Horizontal Dia. Before the Test

D_H' : Horizontal Dia. After the Test

Table 3.10 Diameters of Pipe in RUN 5504

		Vertical Dia.			Horizontal Dia.		
L		D_V	D_V'	$D_V'-D_V$	D_H	D_H'	$D_H'-D_H$
1	650	113.85	113.81	-0.04	114.97	114.81	-0.16
2	750	114.47	114.14	-0.33	113.64	113.81	0.24
3	850	114.85	111.52	-3.33	113.31	116.24	2.93
4	950	114.19	101.82	-12.37	114.35	125.42	11.07
5	1050	114.20			114.20	128.45	14.25
6	1150	114.21			114.26	154.20	39.94
7	1250	114.23			114.23	145.50	31.27
8	1350	114.18	103.05	-11.13	114.15	124.00	9.85
9	1450	114.12	112.45	-1.67	114.16	116.02	1.86
10	1550	114.02	113.55	-0.47	114.22	114.65	0.43
11	1650	114.52	114.38	-0.14	113.26	113.82	0.56
12	1750	114.42	114.40	-0.02	113.65	113.78	0.13
13	1850	114.12	114.29	0.17	114.26	115.39	1.13
14	2800	114.03	114.27	0.24	114.22	115.17	0.95
15	2900	114.21	112.94	-1.27	113.96	116.28	2.32
16	3000	114.18	107.71	-6.47	114.02	118.62	4.6

D_V, D_V' : Vertical Dia. Before or After the Test

D_H, D_H' : Horizontal Dia. Before or After the Test

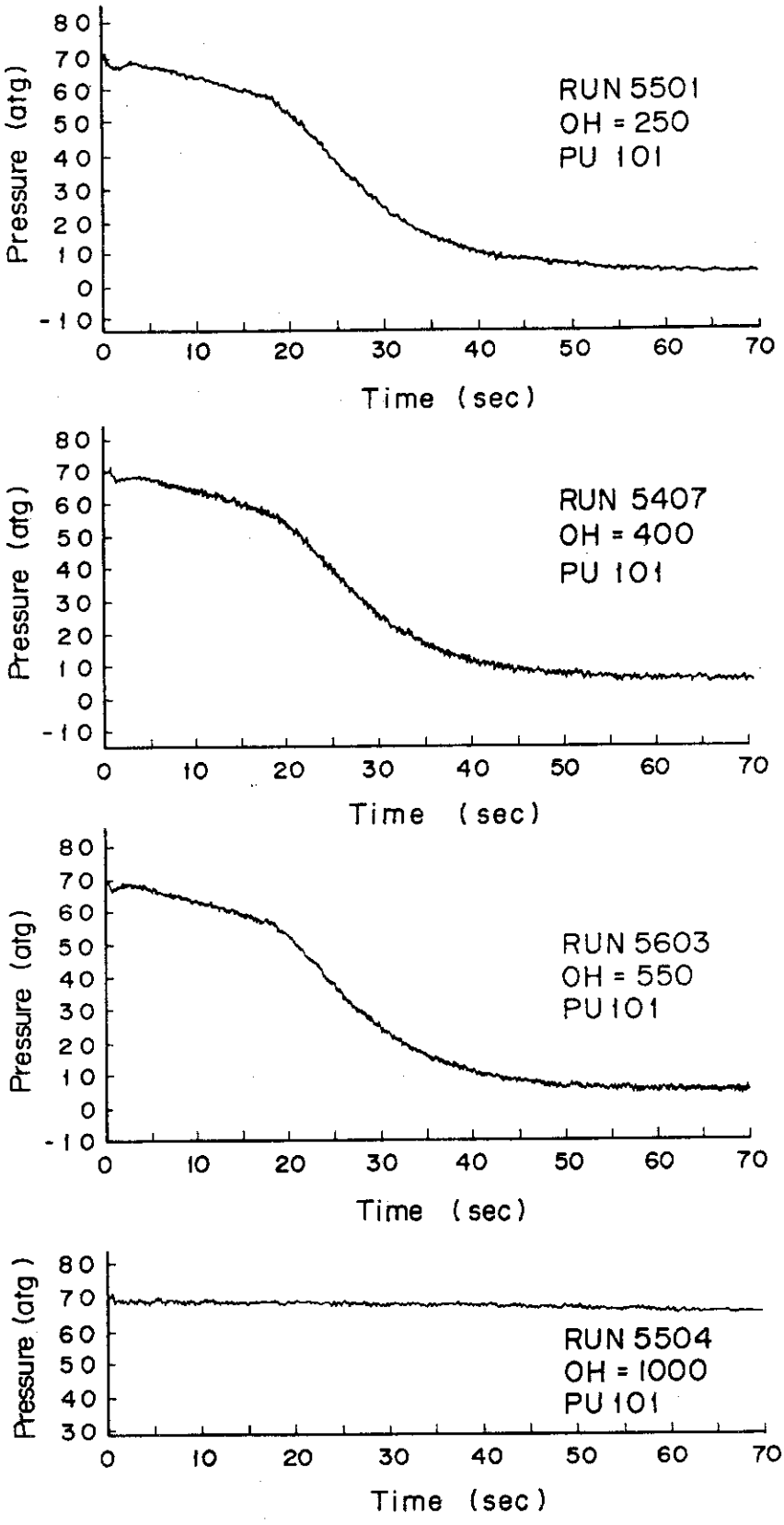

Fig.3.1 Pressure Time Histories in Pressre Vessel

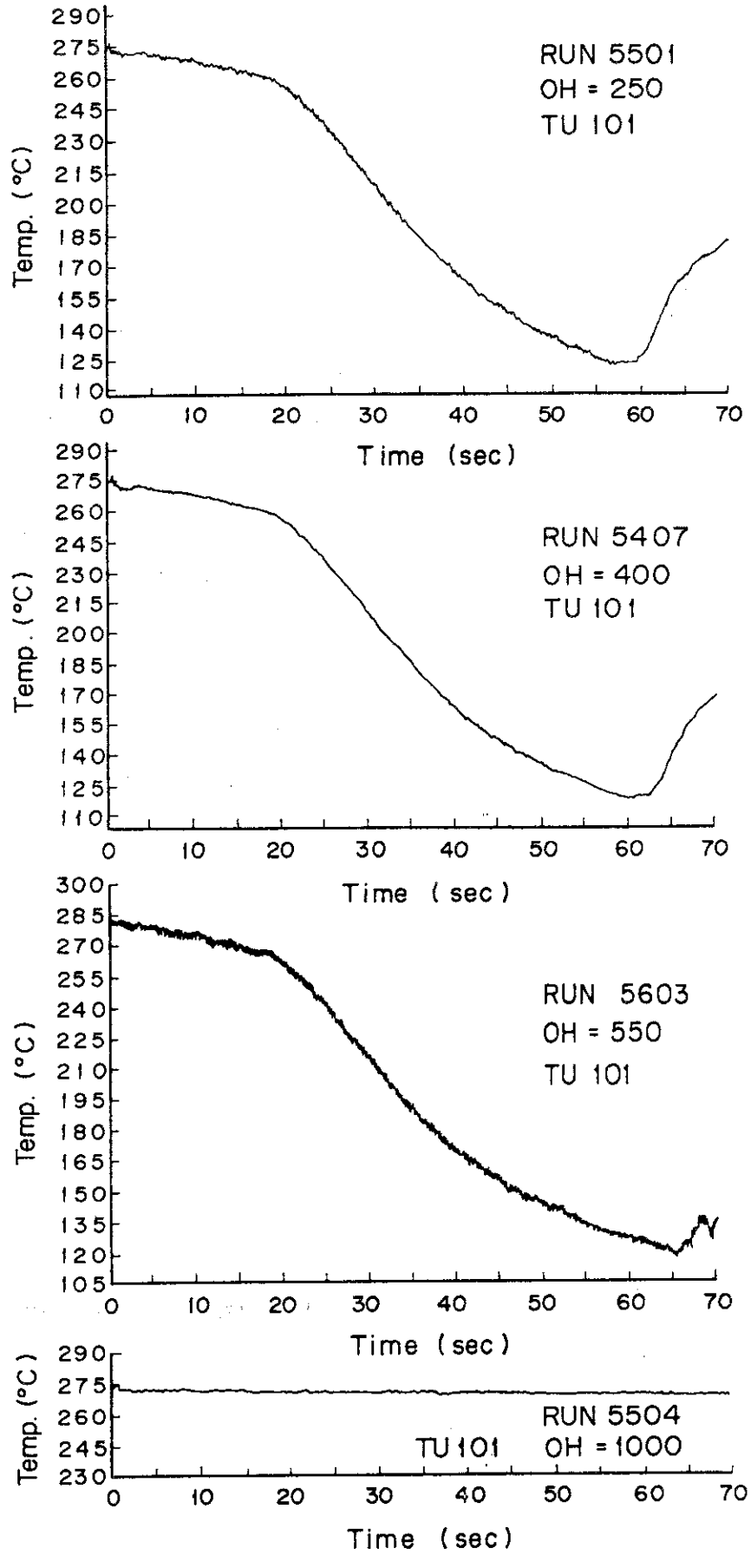

Fig.3.2 Temperature Time Histories in Pressure Vessel

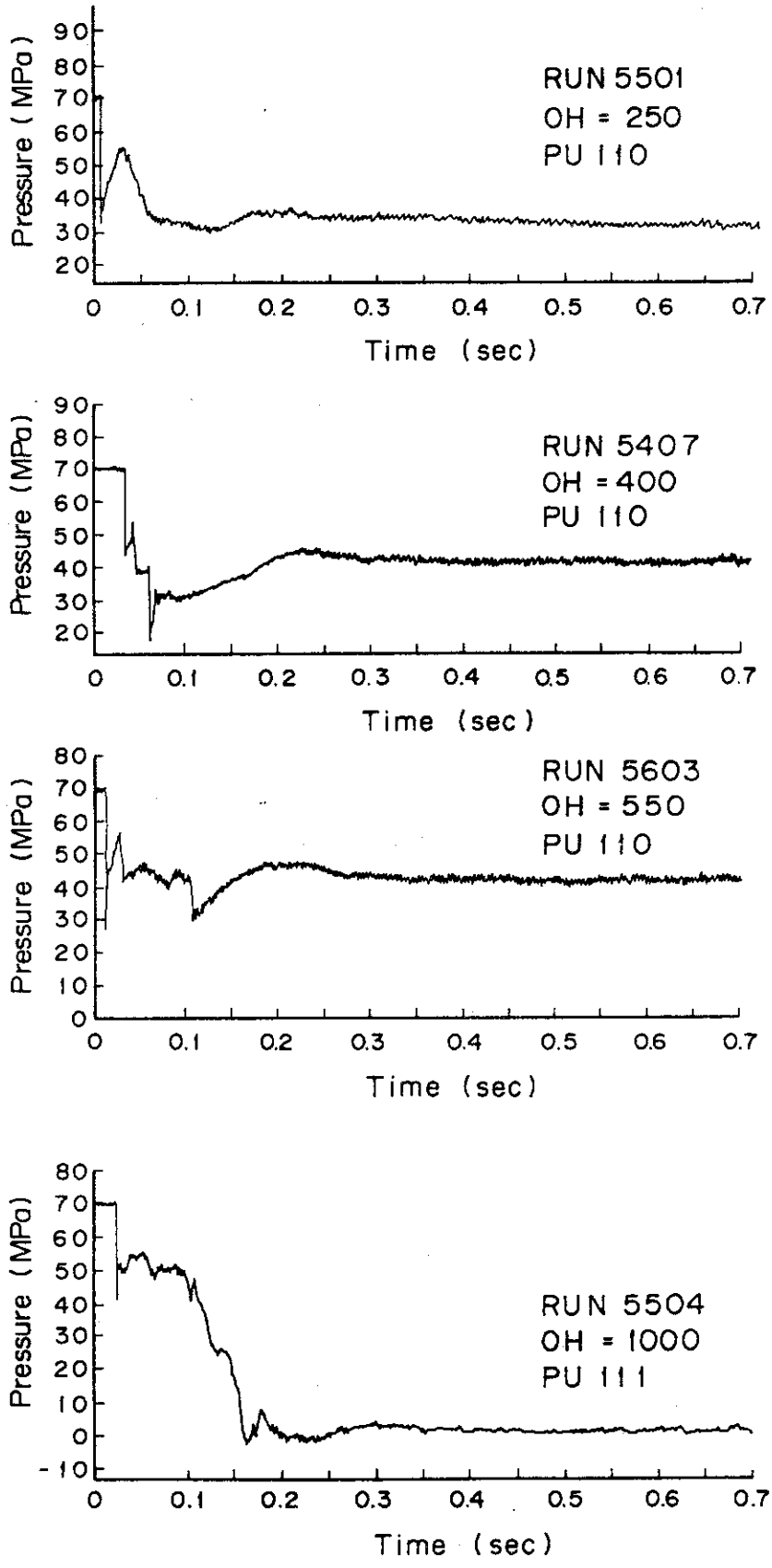

Fig.3.3 Pressure Time Histories in Test Pipe

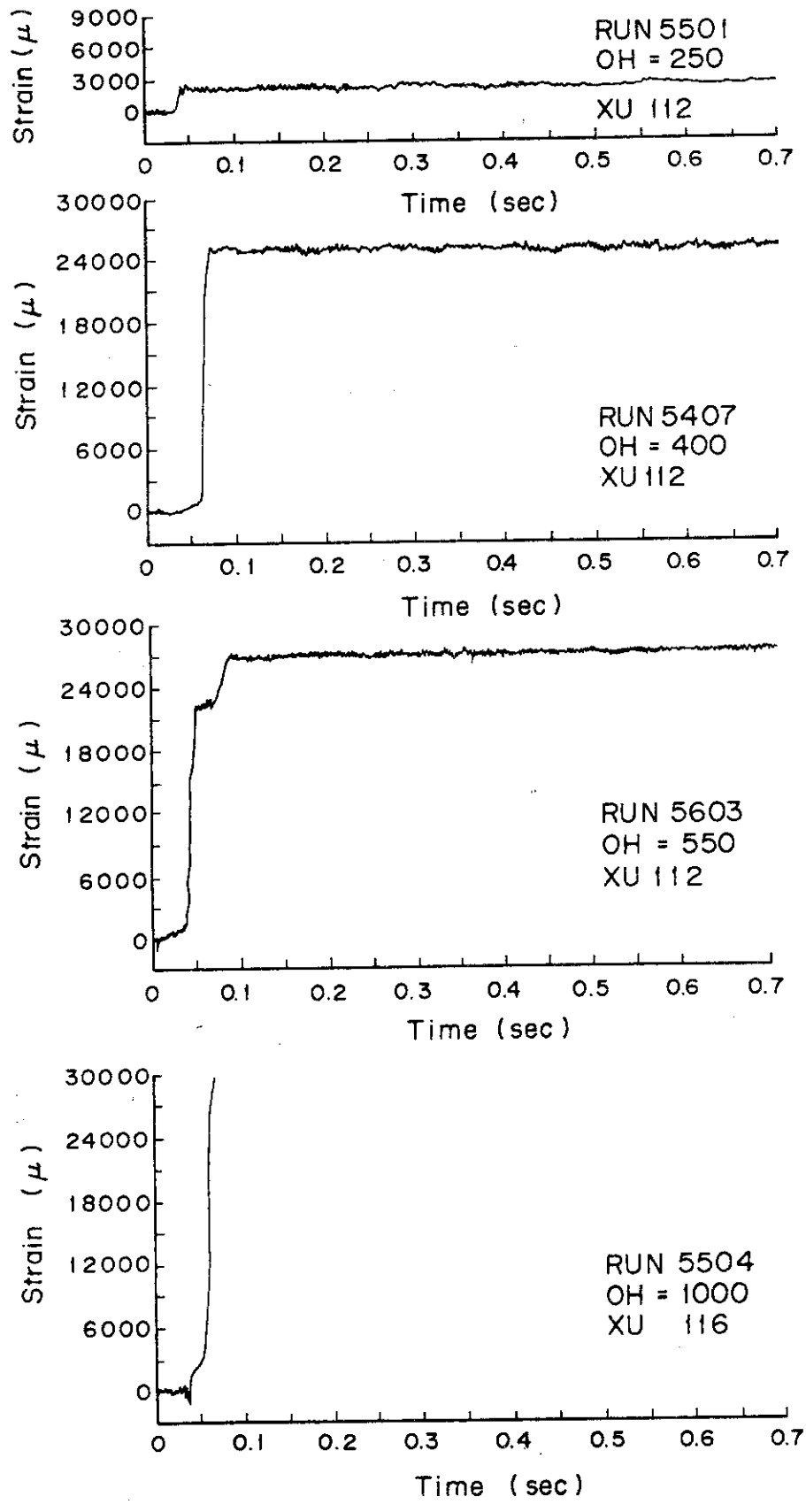

Fig.3.4 Strain of Pipe at a Setting Point of Restraint

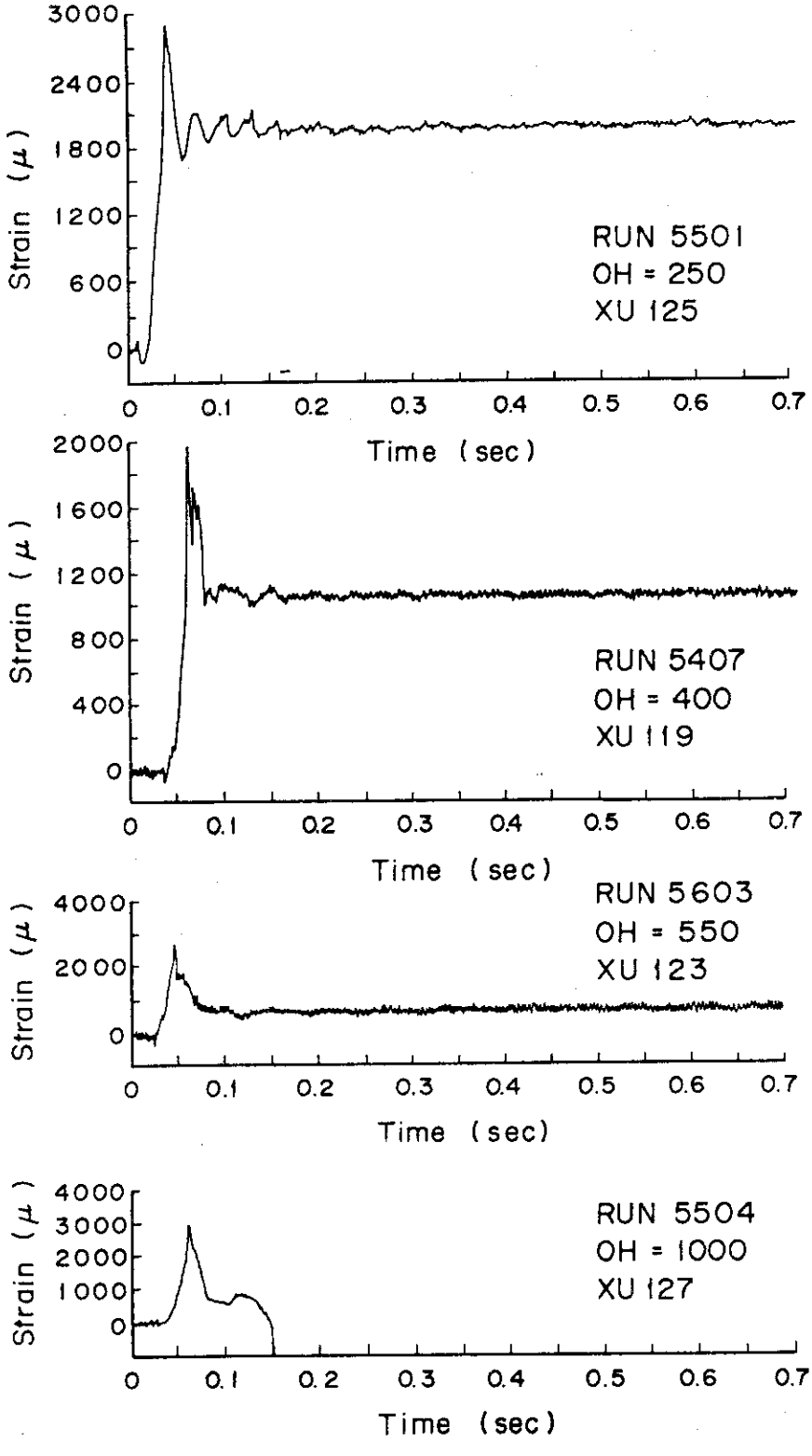

Fig.3.5 Strain of Pipe at a Point near the Pipe Support

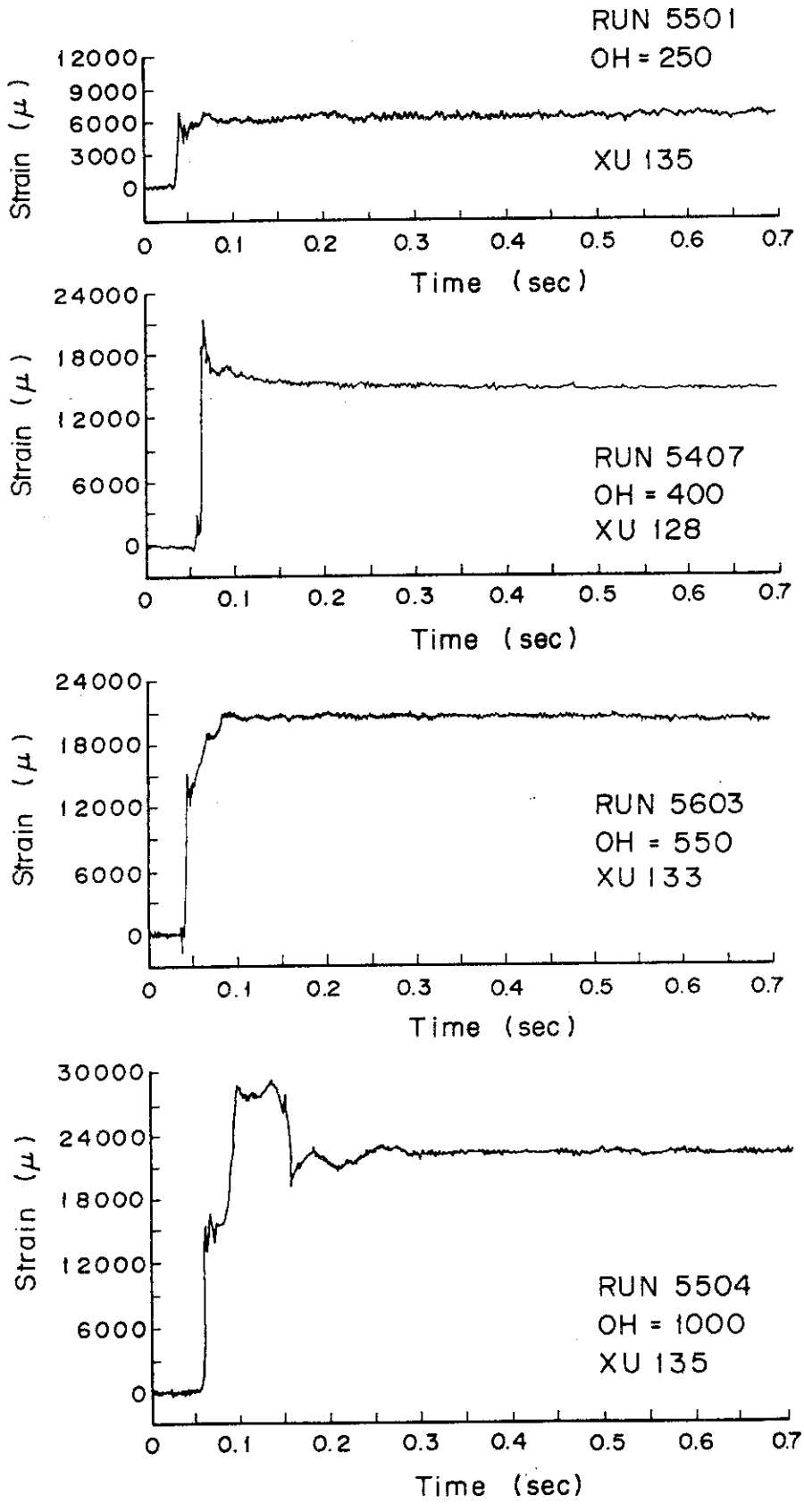

Fig.3.6 Strain of Restraint at a Point of U-bar Straight Portion

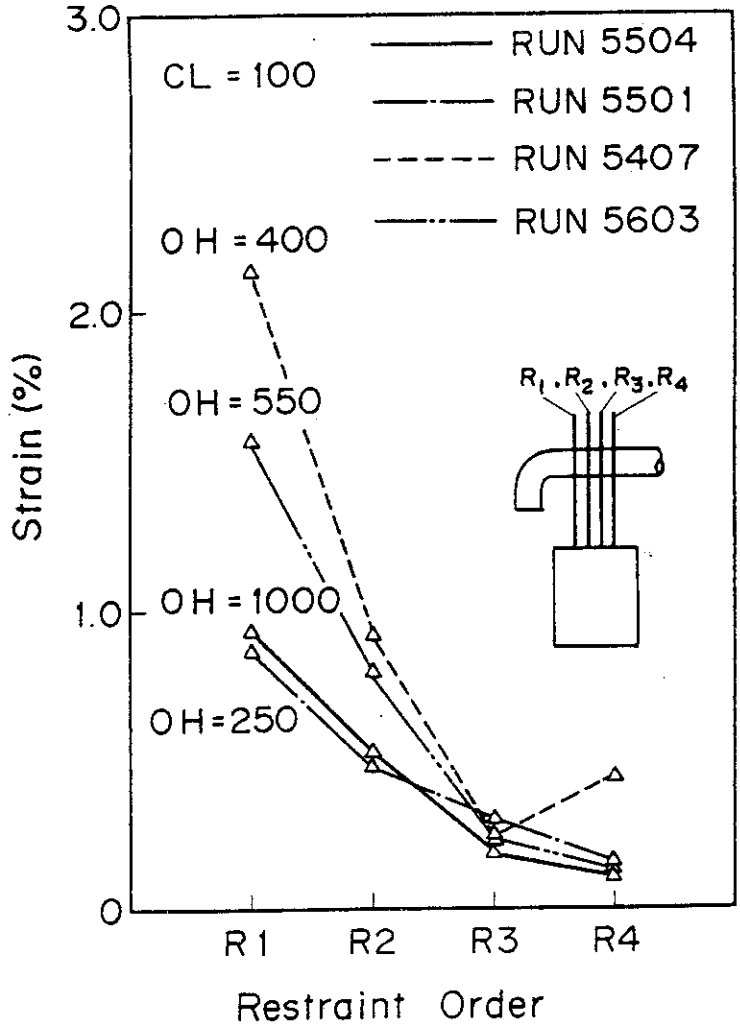

Fig.3.7 Peak Strain of Each Restraint R_1 ,R_2,R_3,R_4

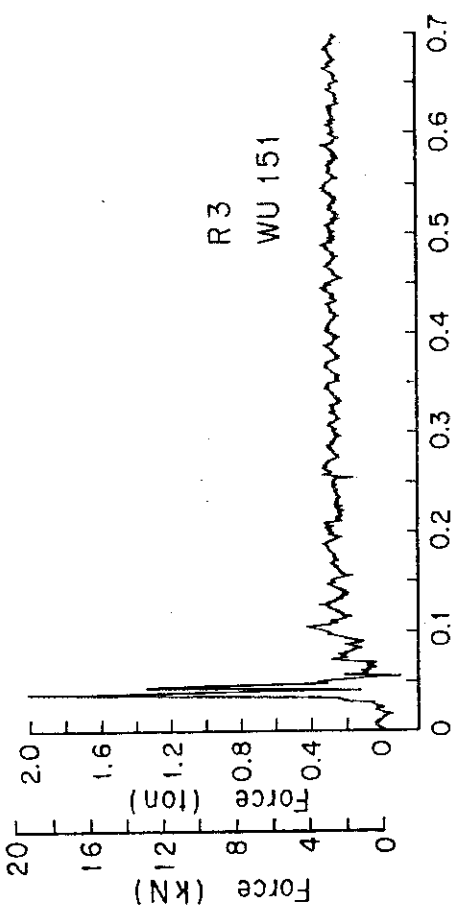

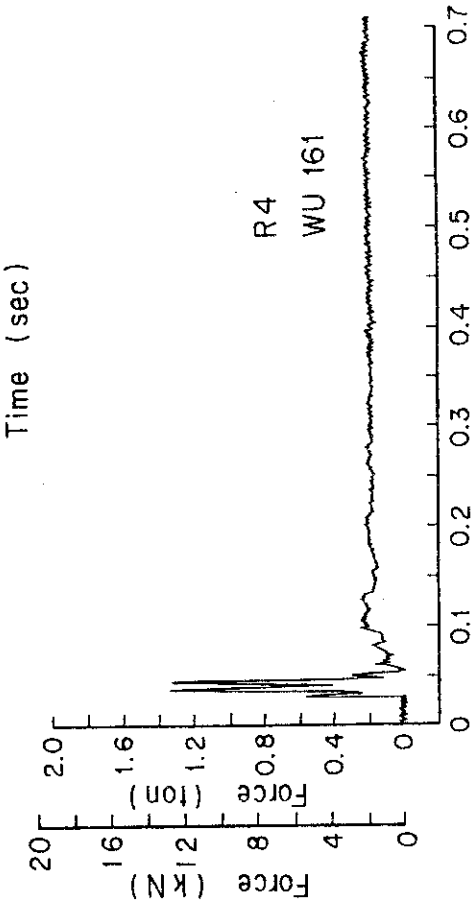

Fig.3.8.2 Restraint Reaction Force in RUN 5501, O H = 250

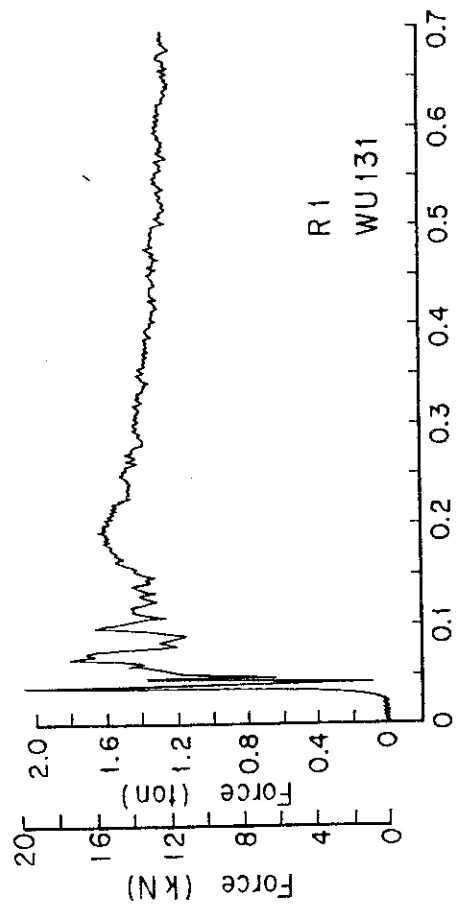

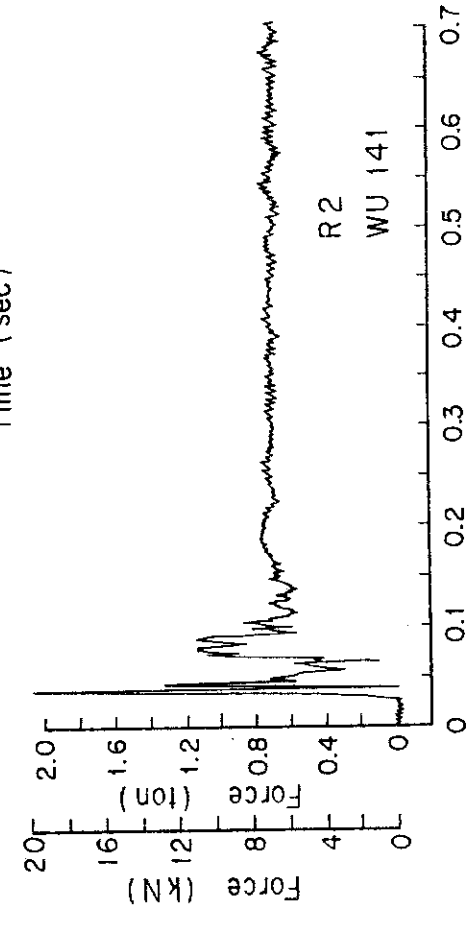

Fig.3.8.1 Restraint Reaction Force in RUN 5501, OH = 250

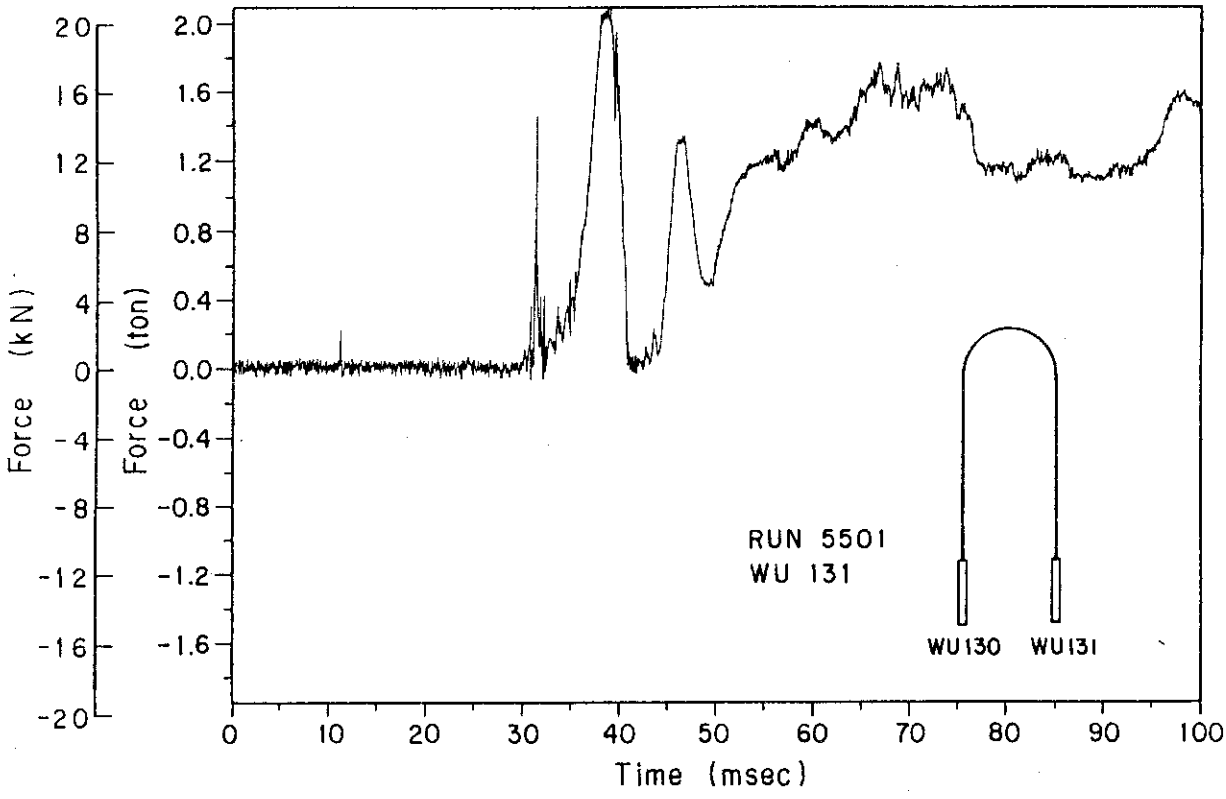

Fig.3.9 Restraint Force of Restraint R_1 (WU131) in RUN 5501

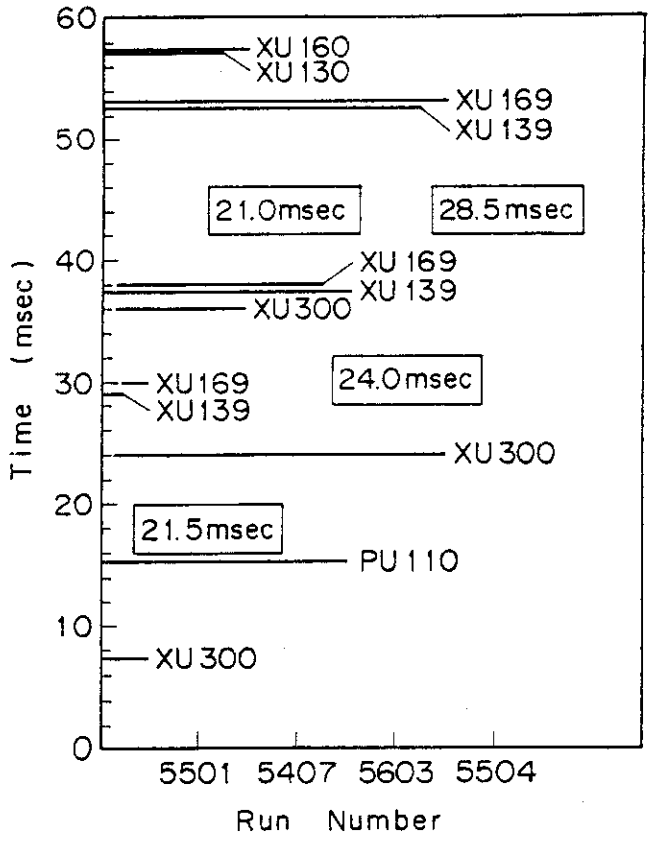

Fig.3.10 Time Sequence of Major Events

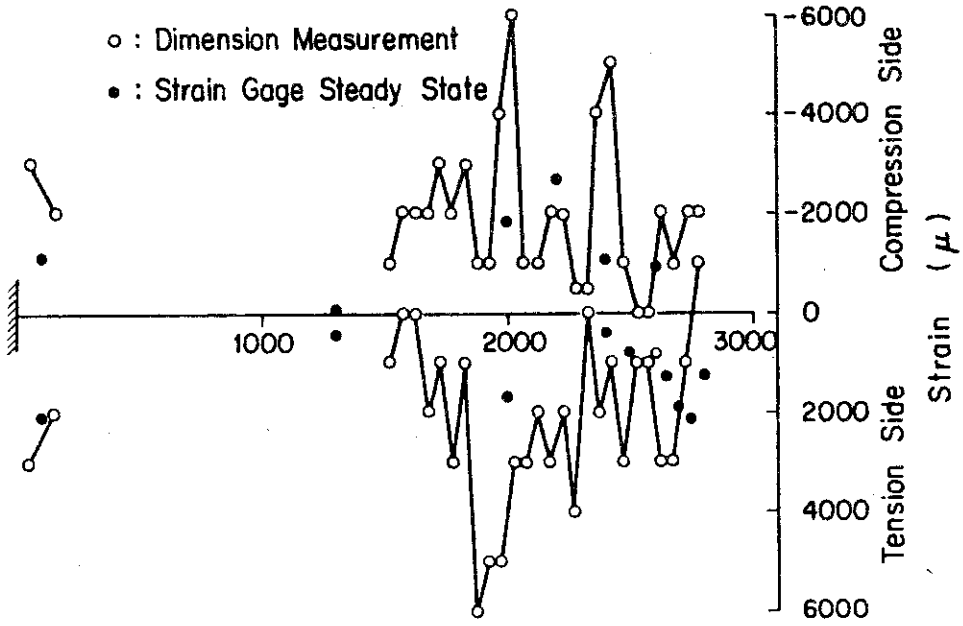

Fig.3.11 Axial Distribution of Pipe Residnal Strains in RUN 5501

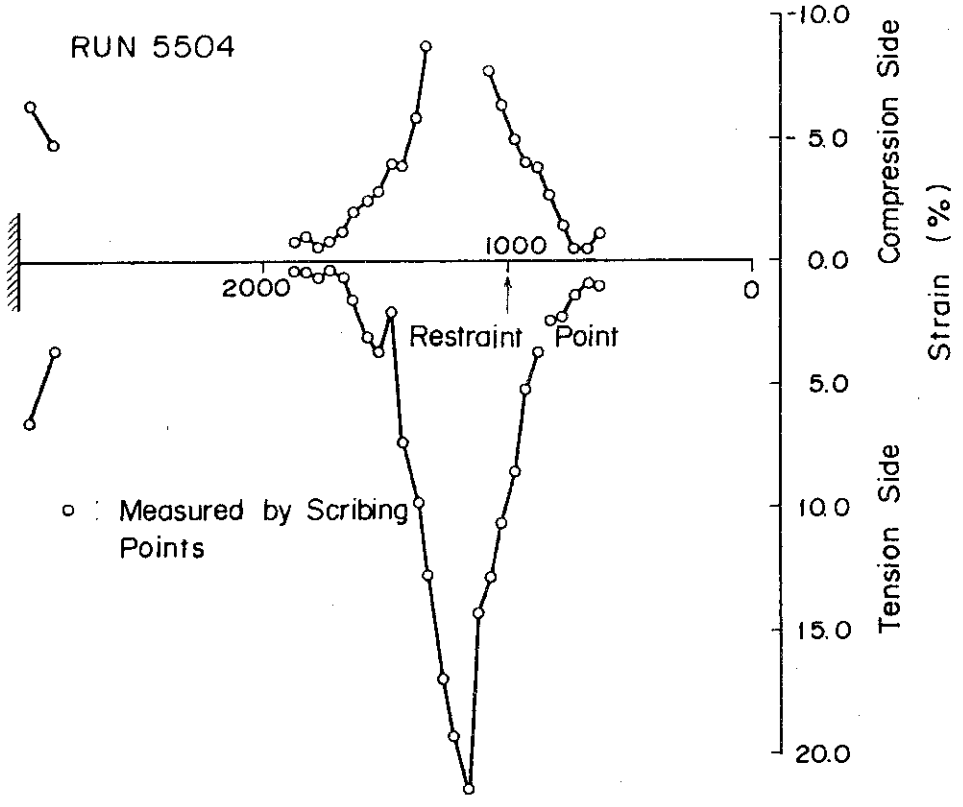

Fig.3.12 Axial Distribution of Pipe Residual Strain in RUN 5504

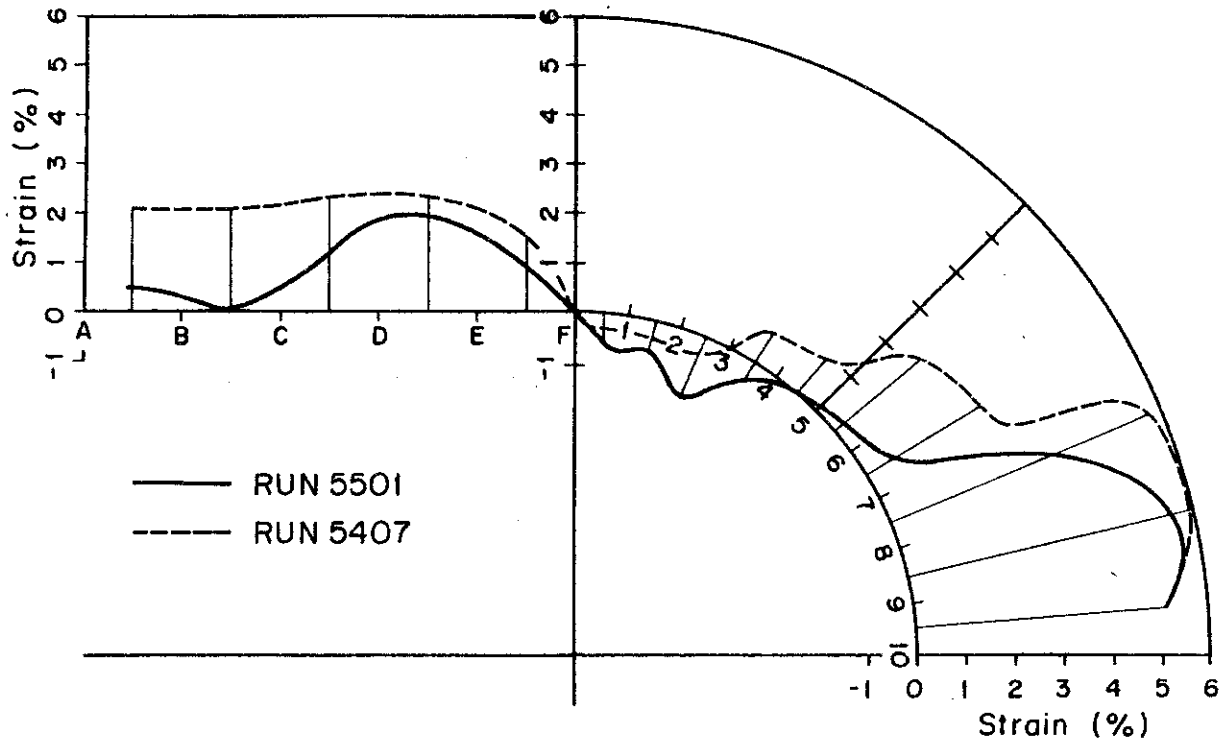

Fig.3.13 Residual Strain of Restraint R_1

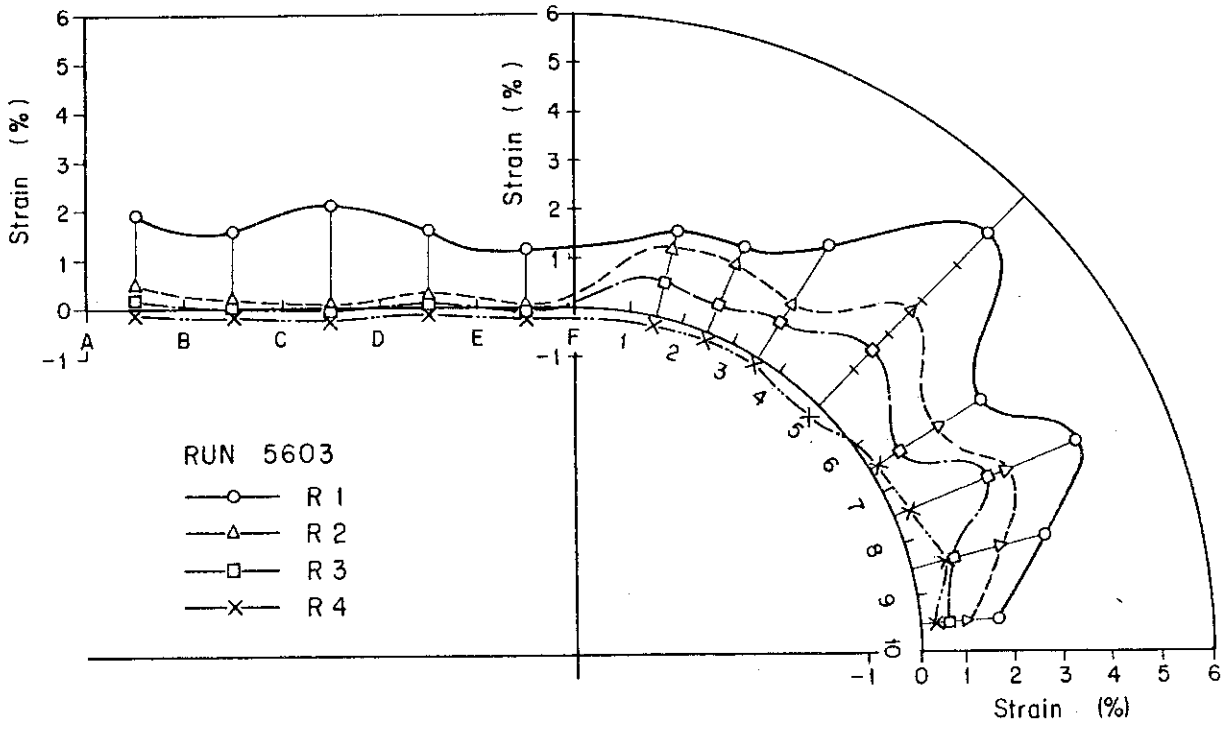

Fig.3.14 Residnal strain of restraint

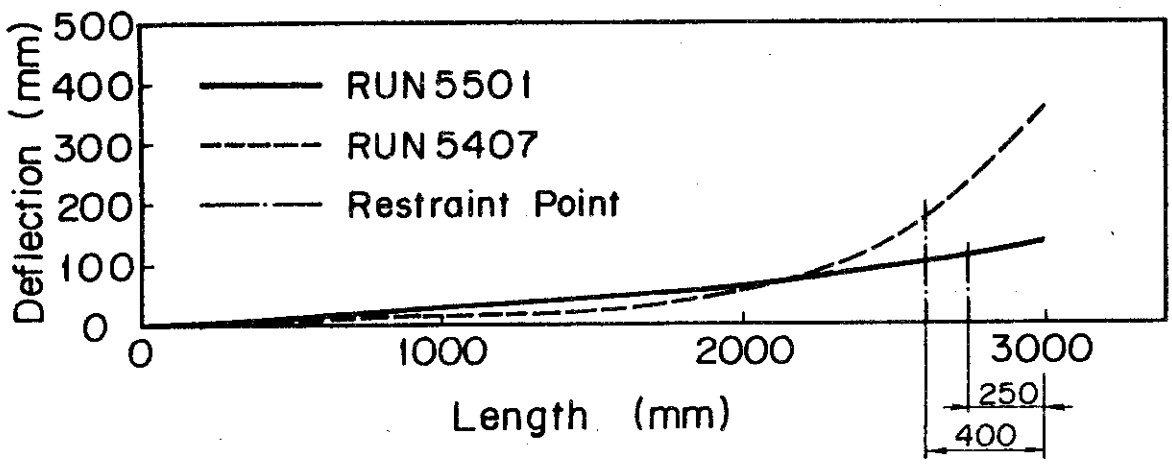

Fig.3.15 Residual Deformation of Pipe

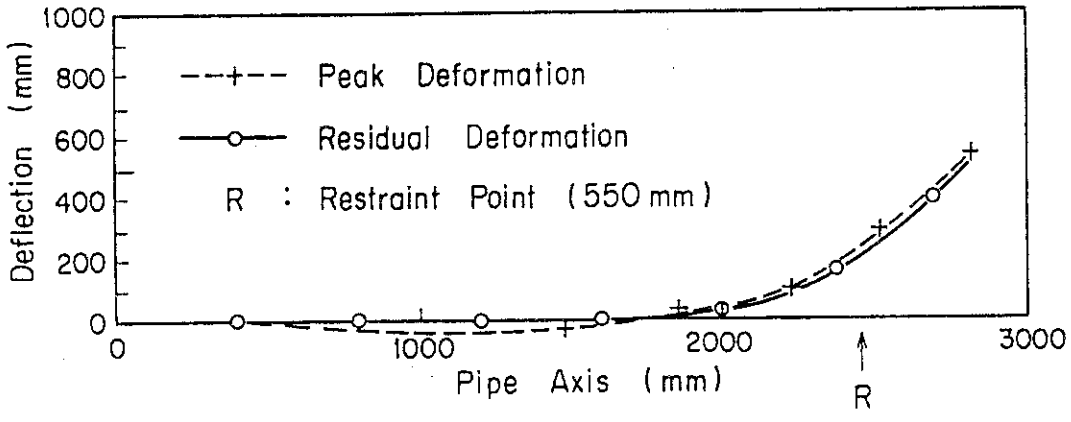

Fig.3.16 Residrial deformation of test pipe

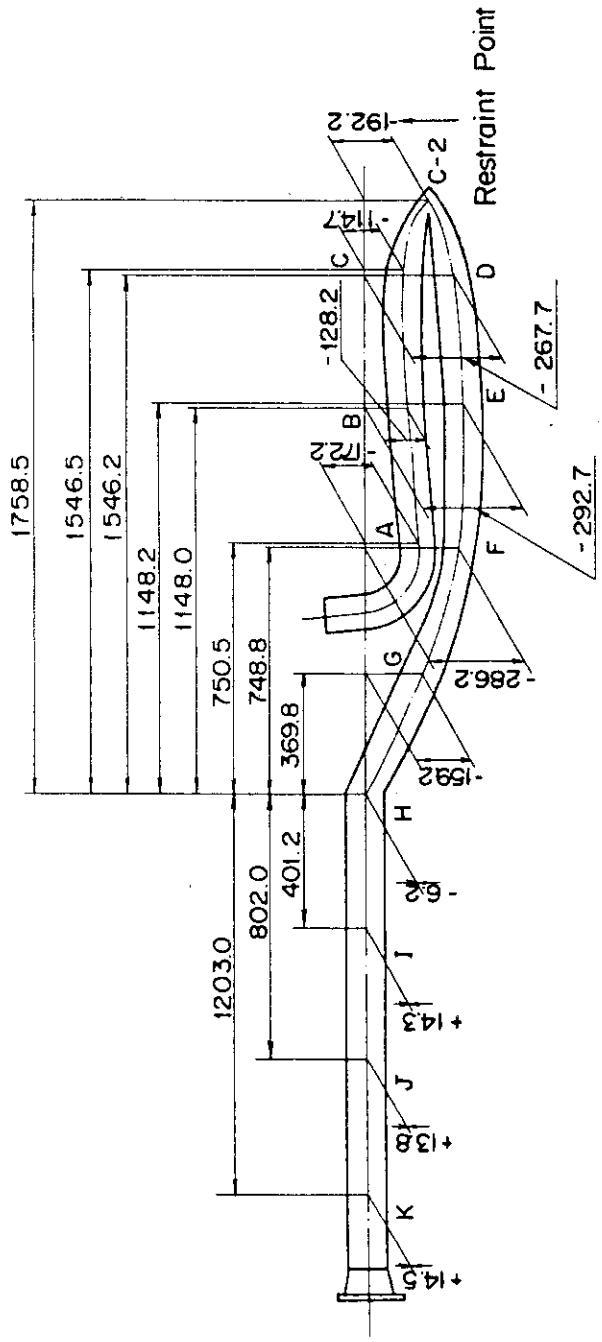

Fig.3.17 Residual Deformation of Test Pipe (RUN 5504)

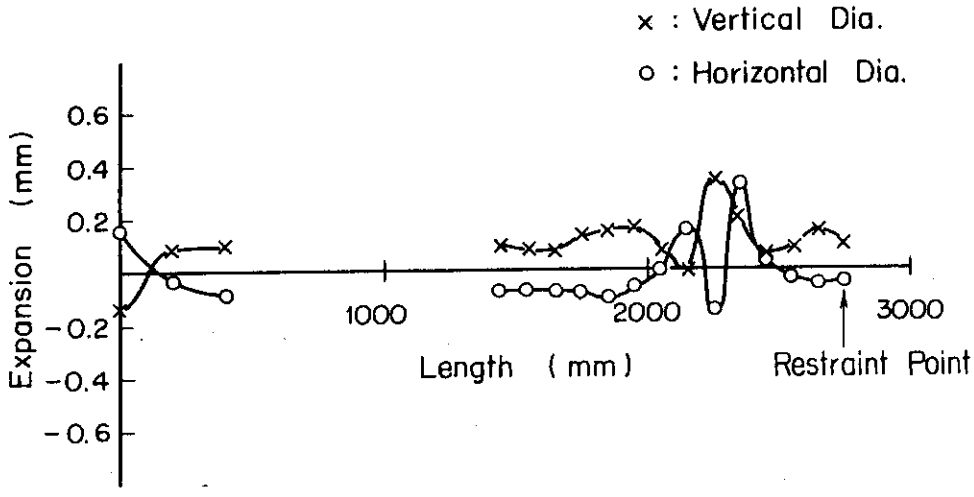

Fig.3.18 Ovallization of Pipe (RUN 5501)

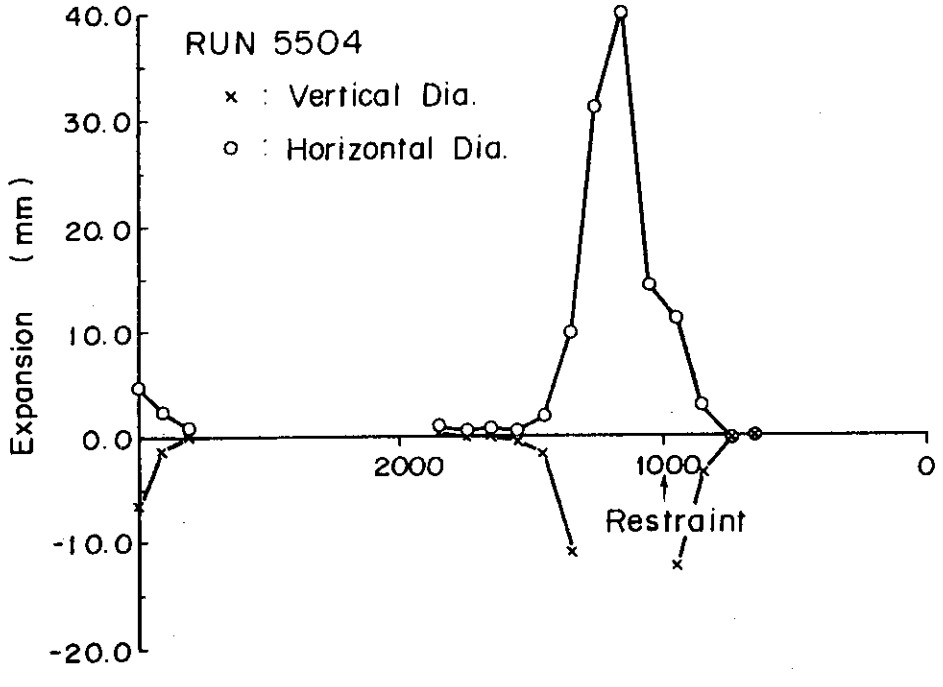

Fig.3.19 Ovallization of Pipe (RUN 5504)

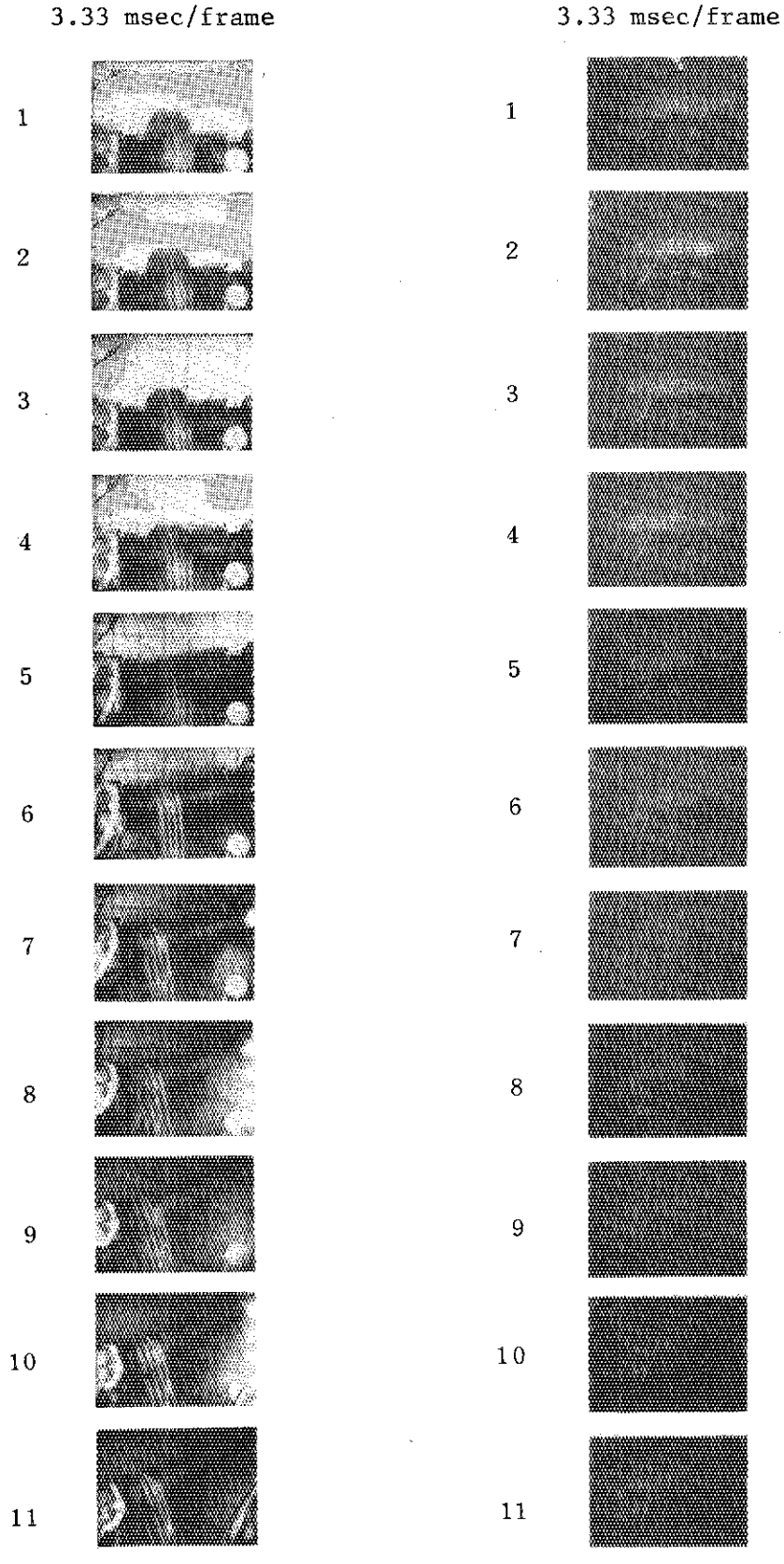

(1) Part (2) Whole

Photo. 3.1 Selected frames of High Speed Camera RUN 5603

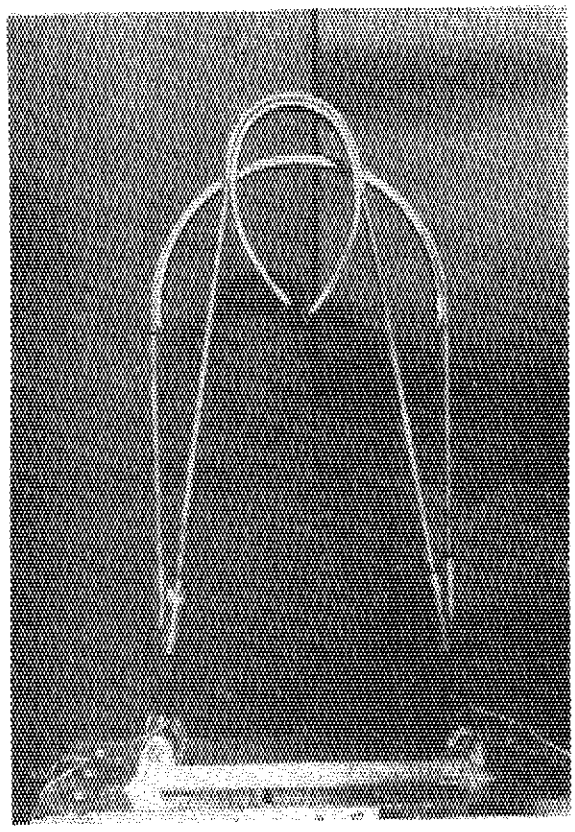

Photo.3.2.1 Restraint R_1 (Front)
RUN 5501

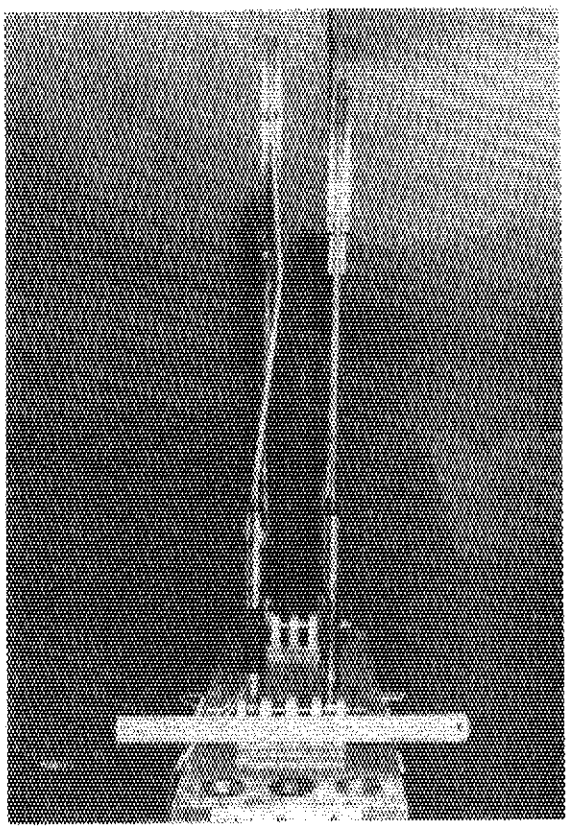

Photo.3.2.2 Restraint F_1 (Side)
RUN 5501

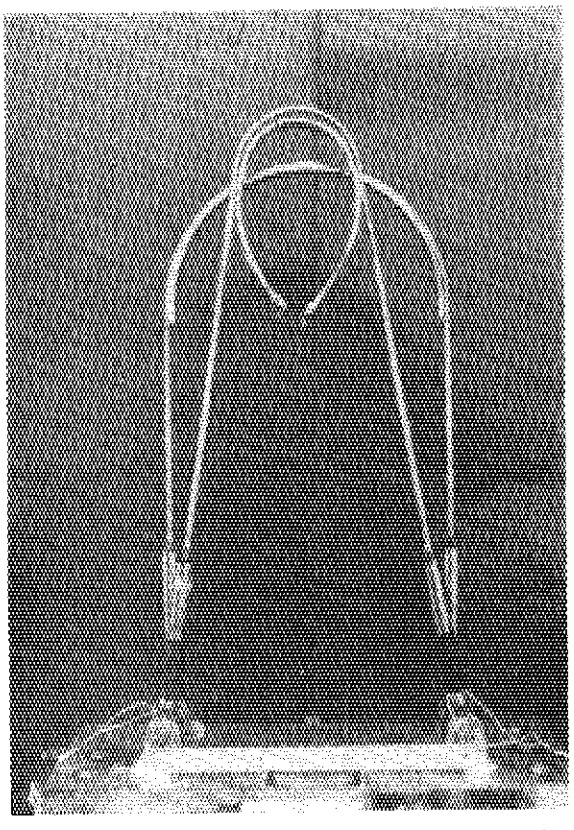

Photo.3.2.3 Restraint R_2 (Front)
RUN 5501

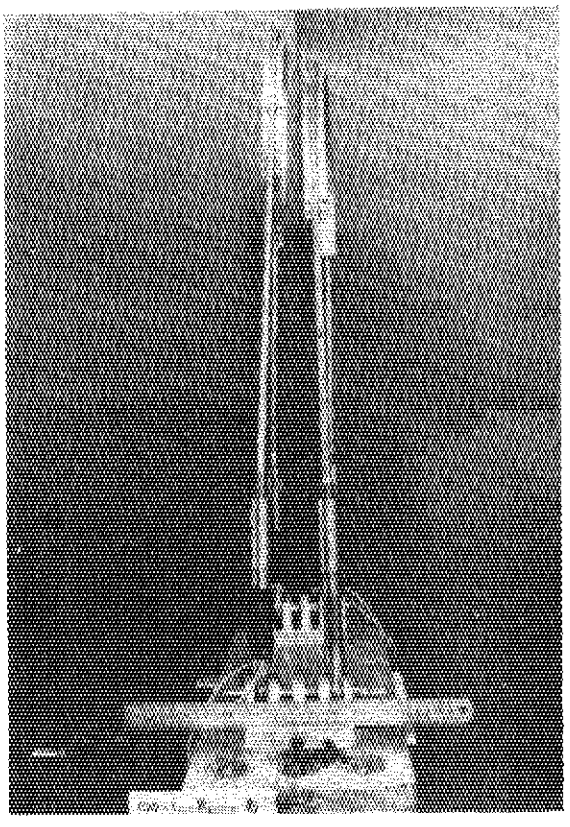

Photo.3.2.4 Restraint R_2 (Side)
RUN 5501

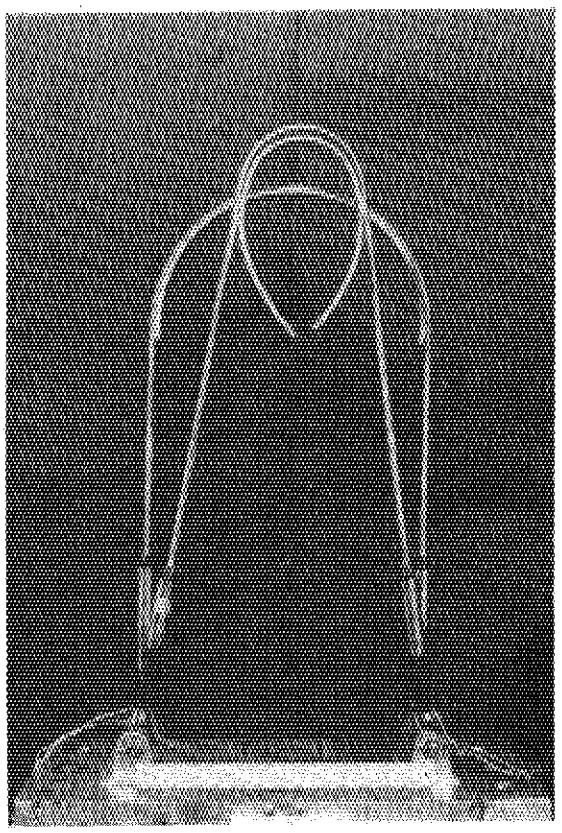

Photo.3.2.5 Restraint R_3 (Front) (RUN 5501)

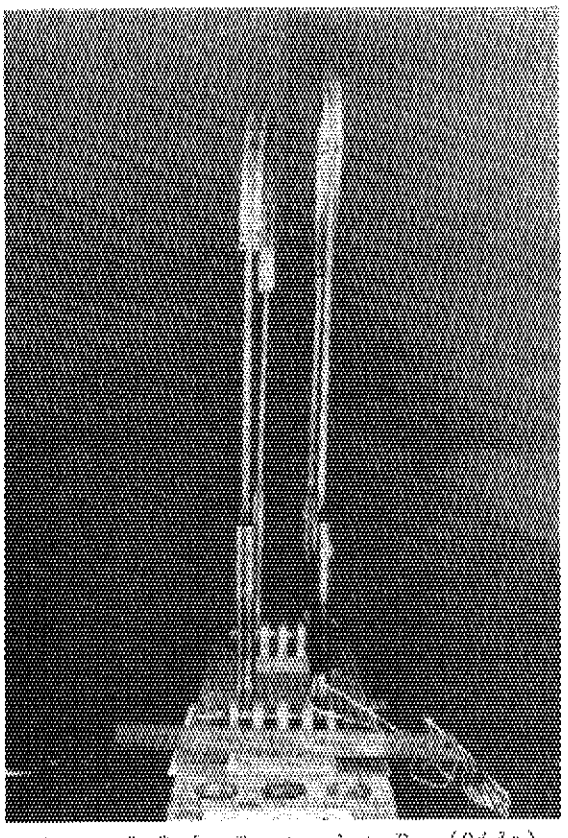

Photo.3.2.6 Restraint R_3 (Side) RUN 5501

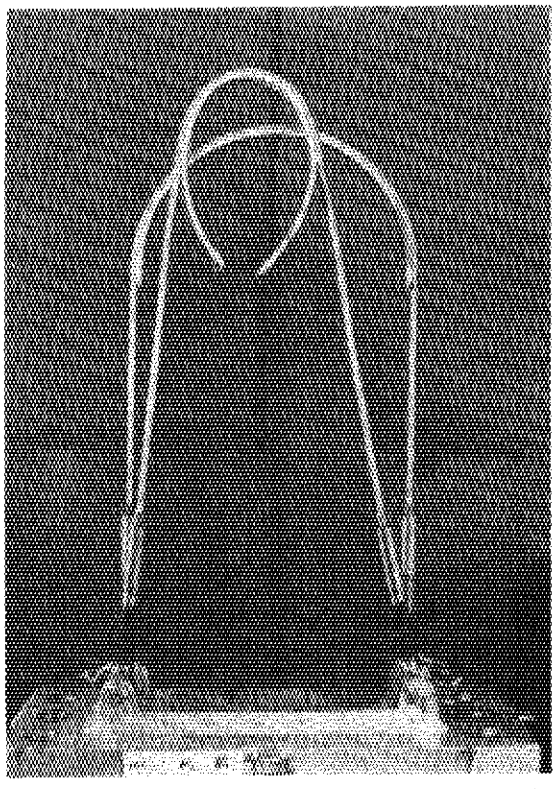

Photo.3.2.7 Restraint R_4 (Front) RUN 5501

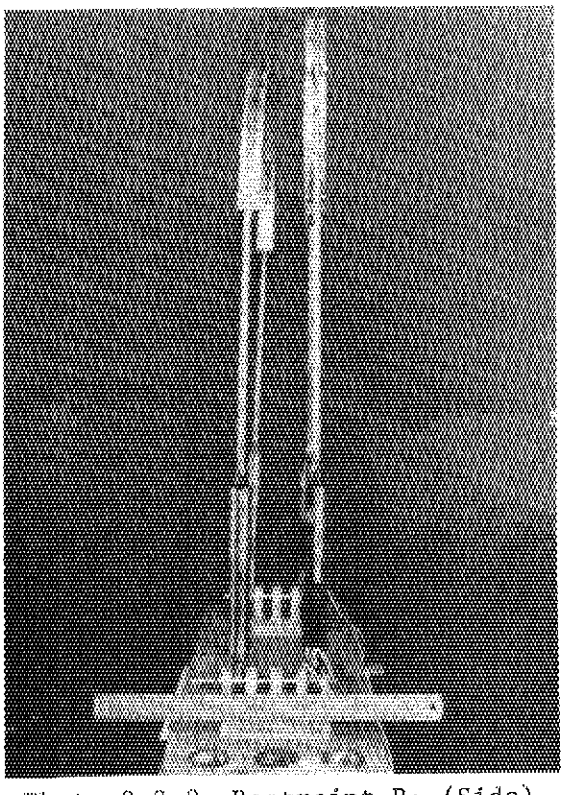

Photo.3.2.8 Restraint R_4 (Side) RUN 5501

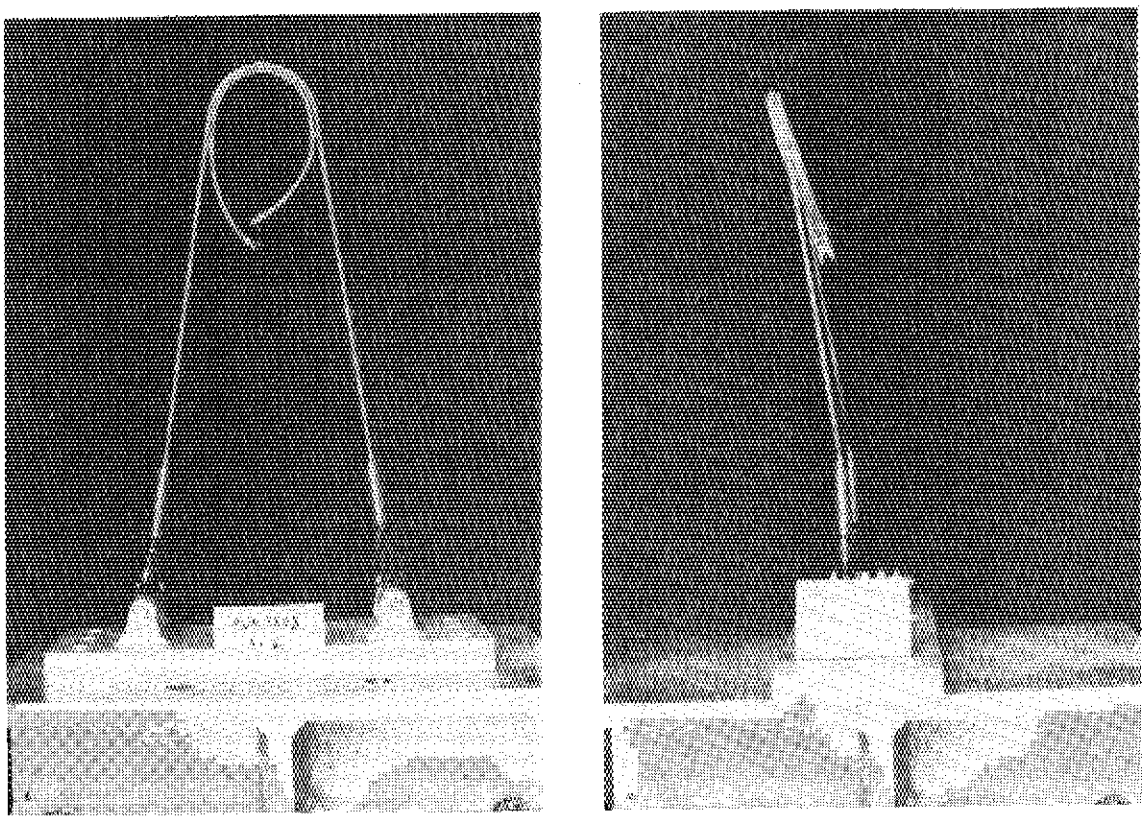

Photo. 3.3.1 View of restraint R1 deformation after test RUN 5603

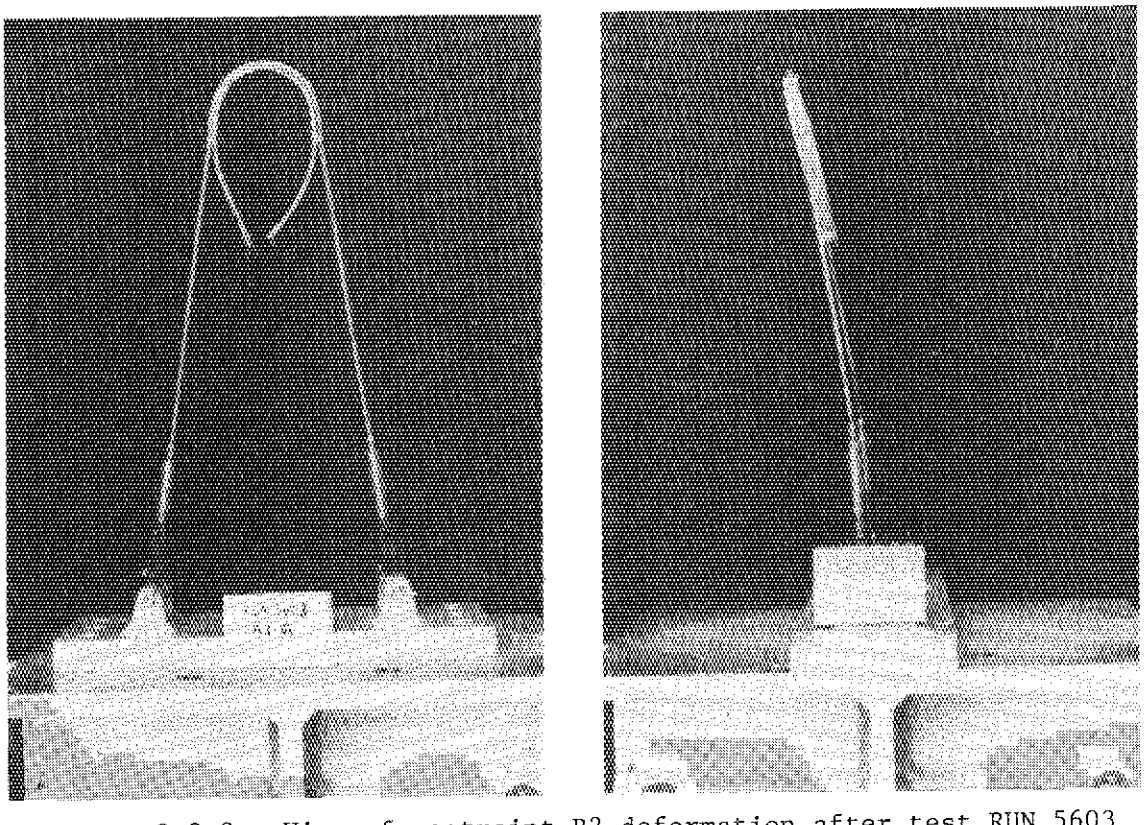

Photo. 3.3.2 View of restraint R2 deformation after test RUN 5603

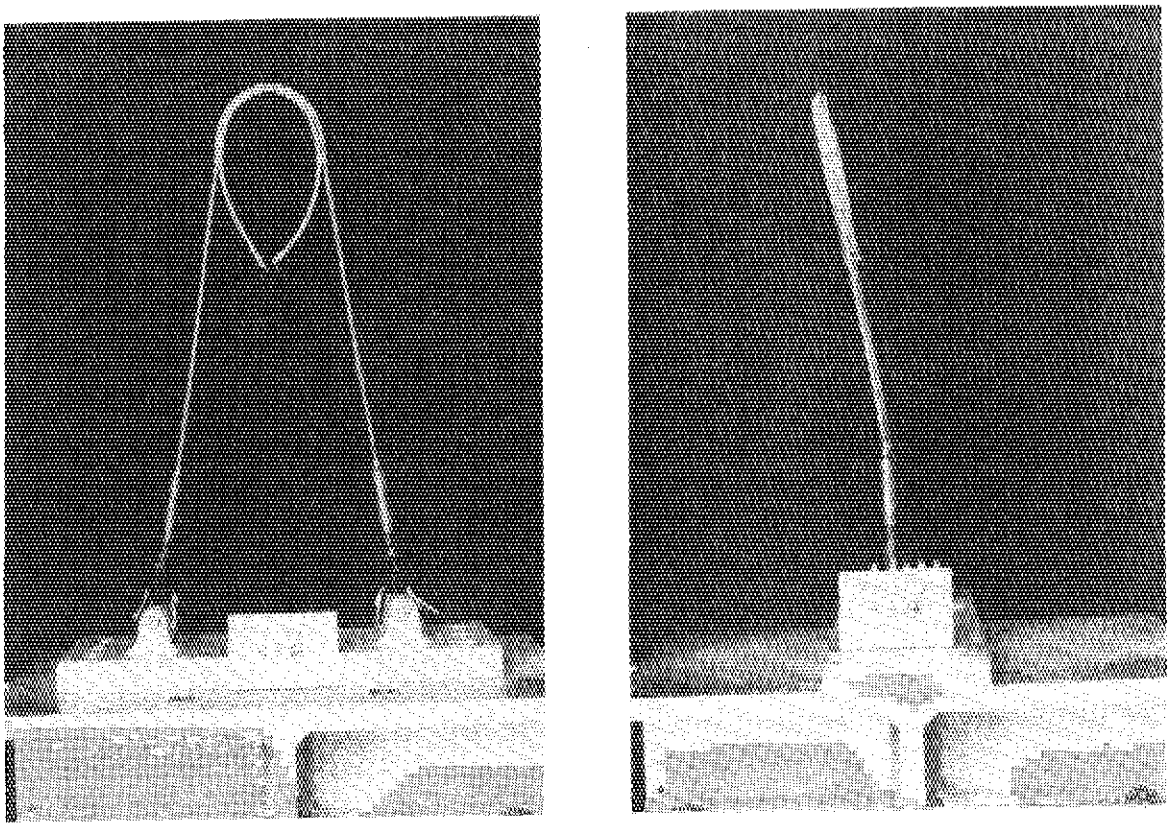

Photo. 3.3.3 View of restraint R3 deformation after test RUN 5603

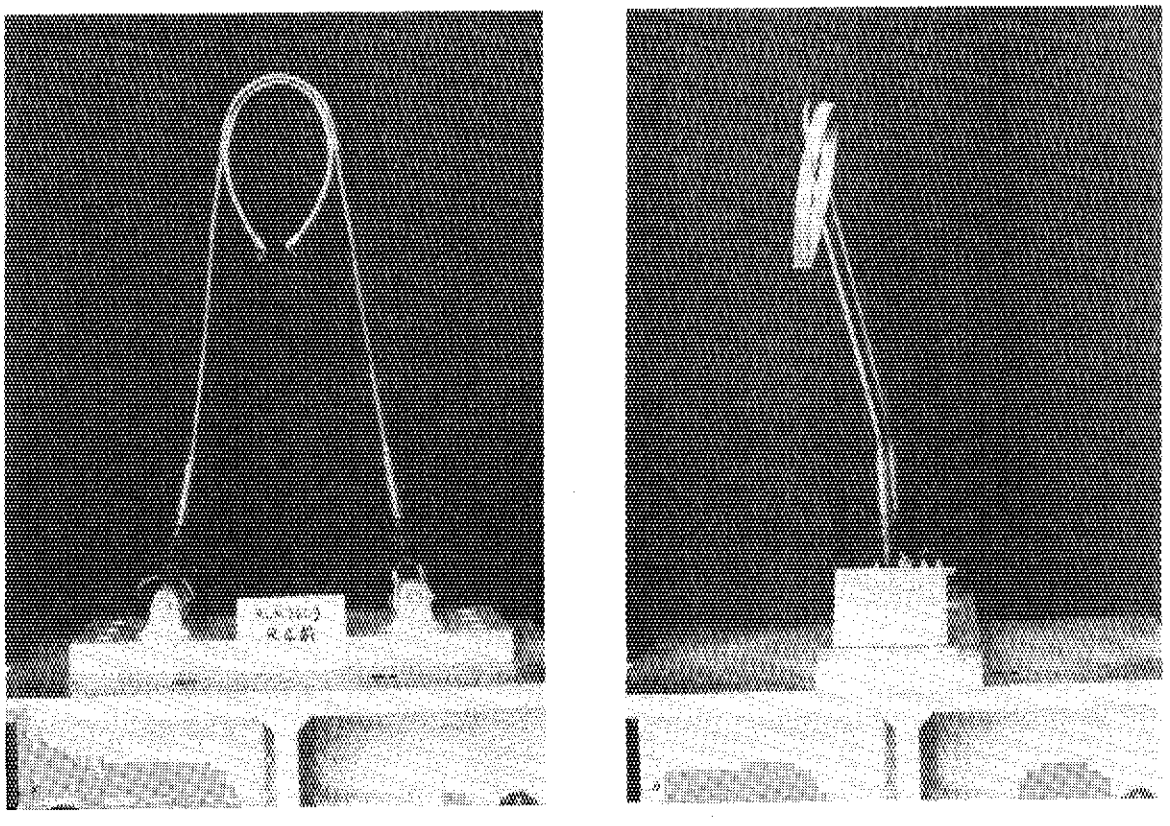

Photo. 3.3.4 View of restraint R4 deformation after test RUN 5603

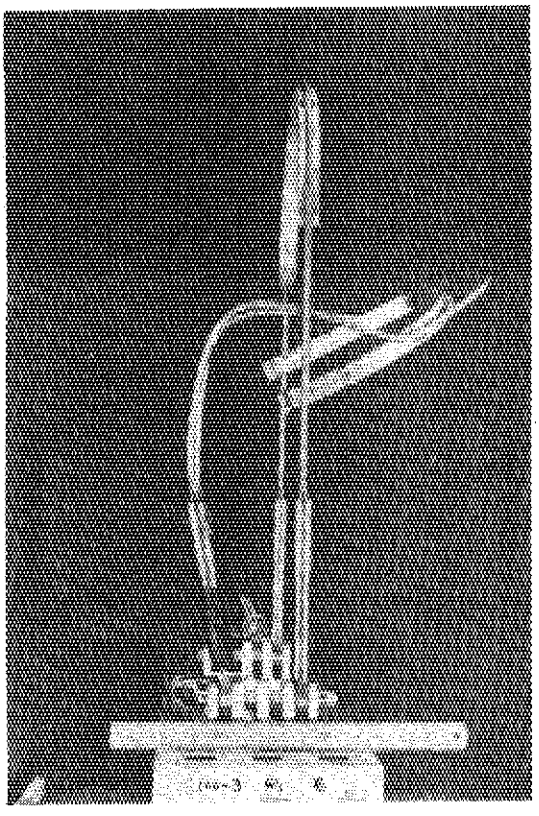

Photo. 3.4.1 RUN 5504, R_1

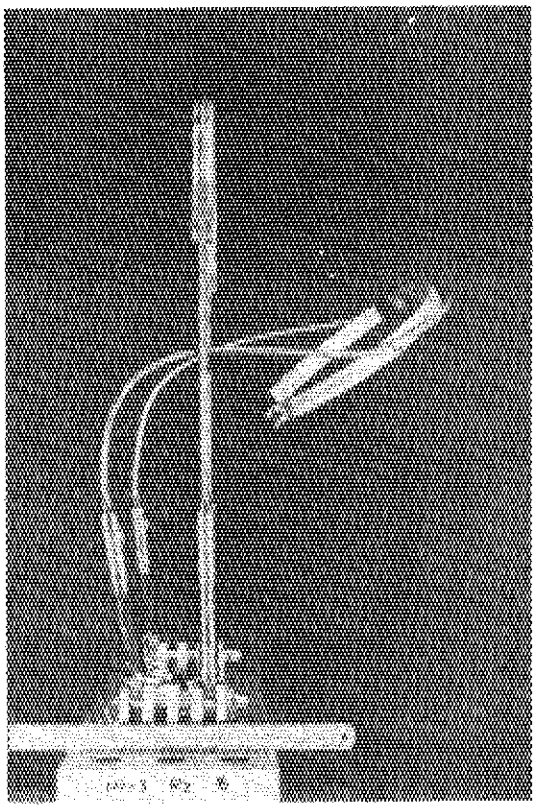

Photo. 3.4.2 RUN 5504, R_2

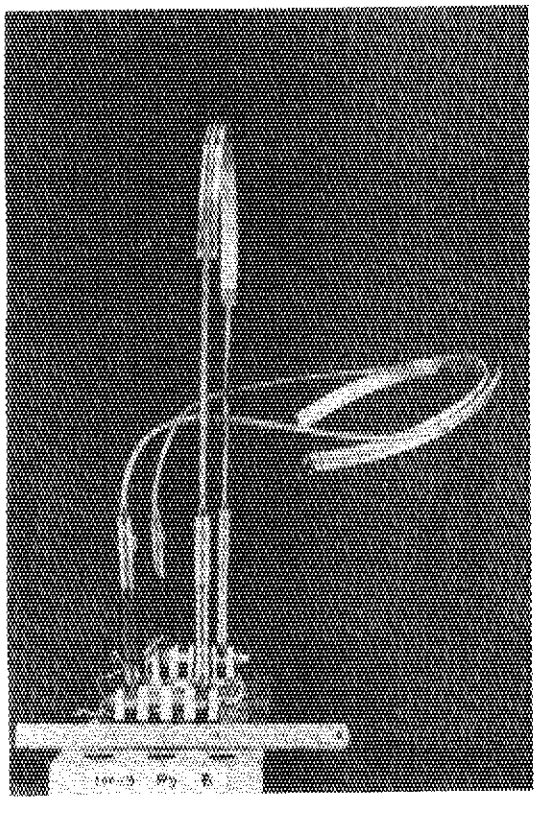

Photo. 3.4.3 RUN 5504, R_3

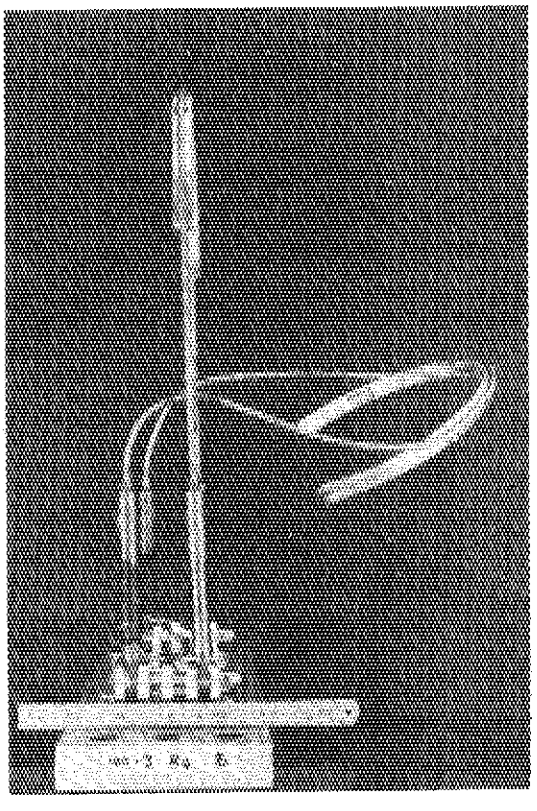

Photo. 3.4.4 RUN 5504, R_4

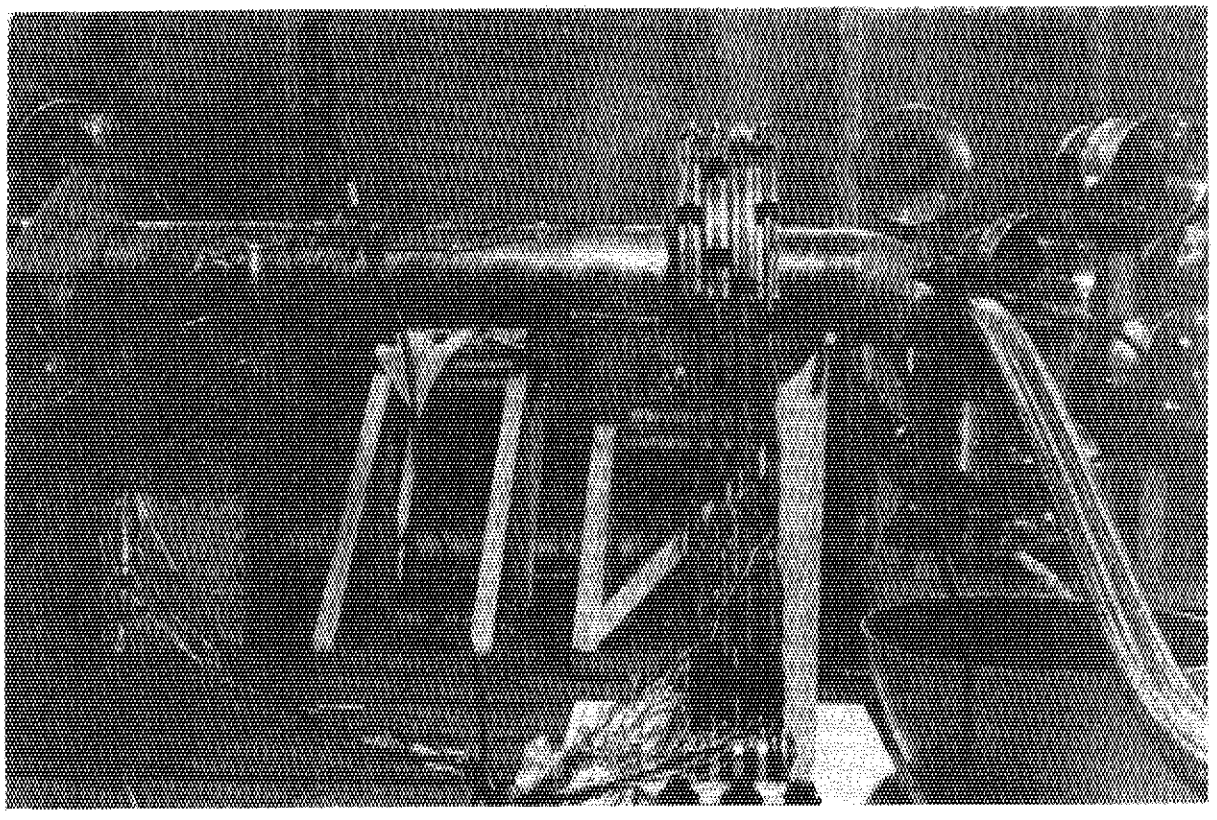

Photo. 3.5.1 View of the pipe and restraint before the test RUN 5501

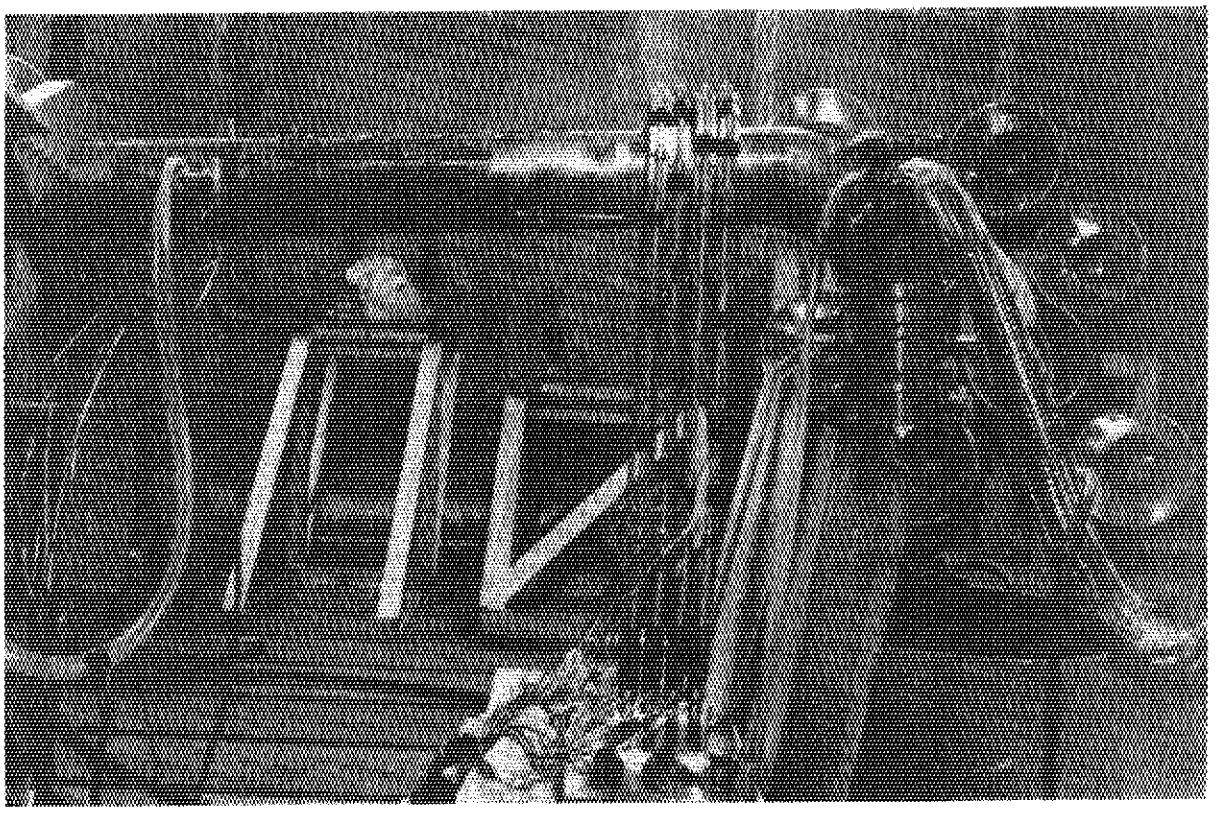

Photo. 3.5.2 View of the pipe and restraint after the test RUN 5501

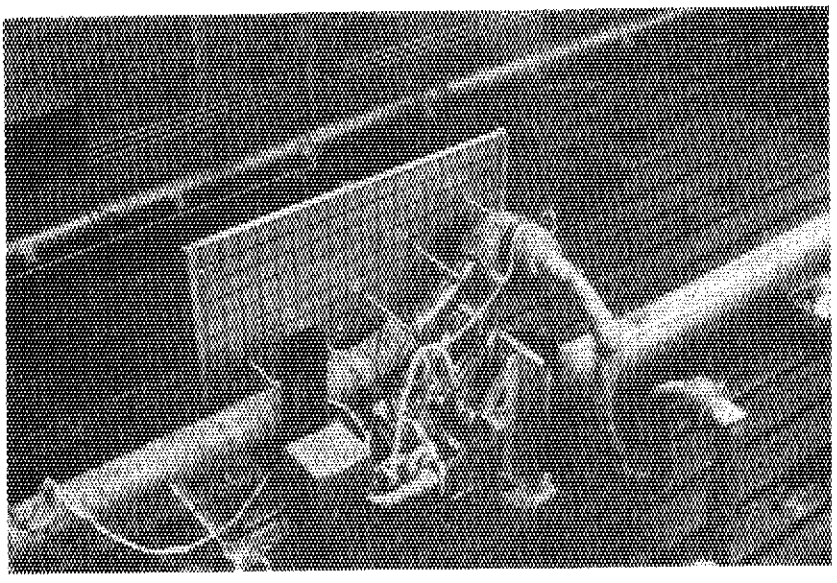

Photo. 3.6.1 View of the test system after test RUN 5603

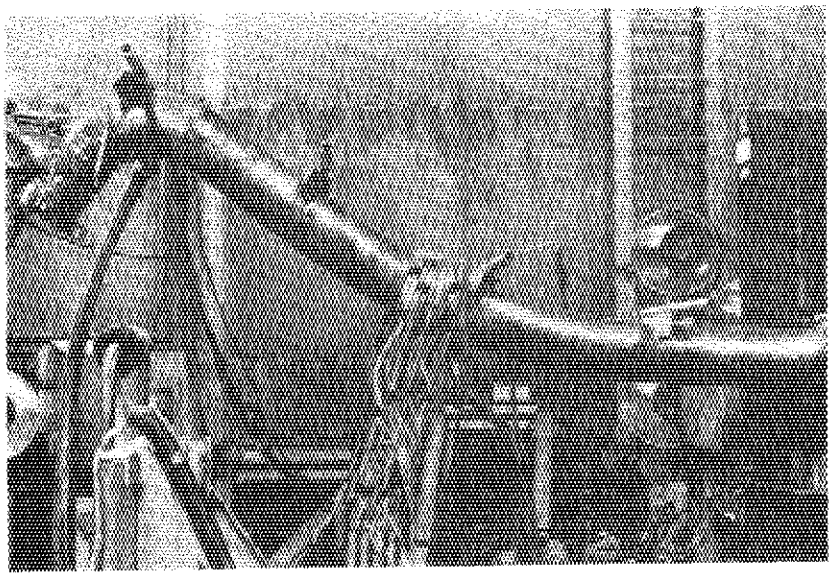

Photo. 3.6.2 Pipe and restraints after test RUN 5603

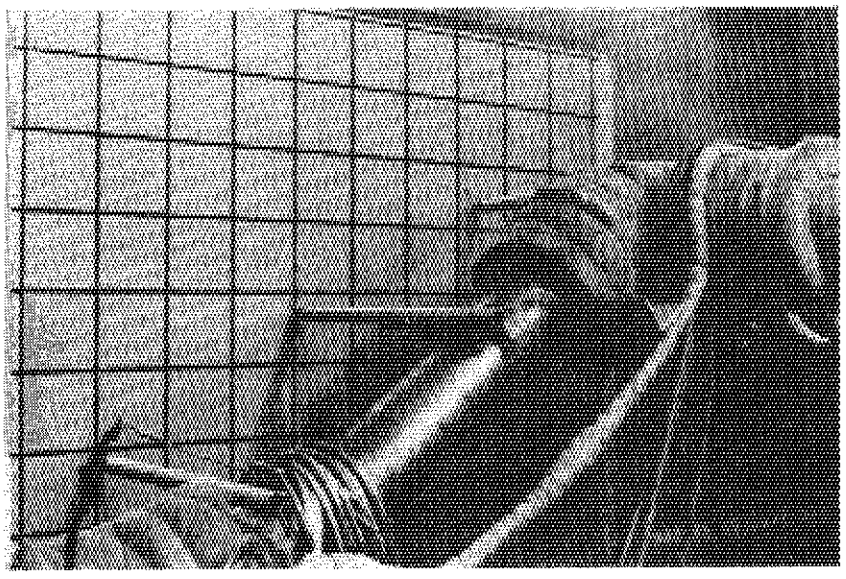

Photo. 3.6.3 Trace of the whipping pipe

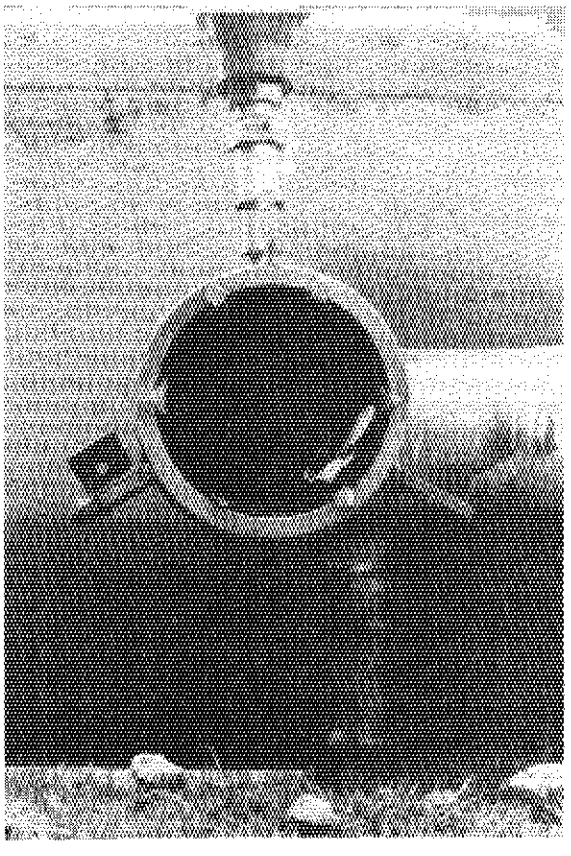

Photo. 3.6.4 Openning situation of rapture disc

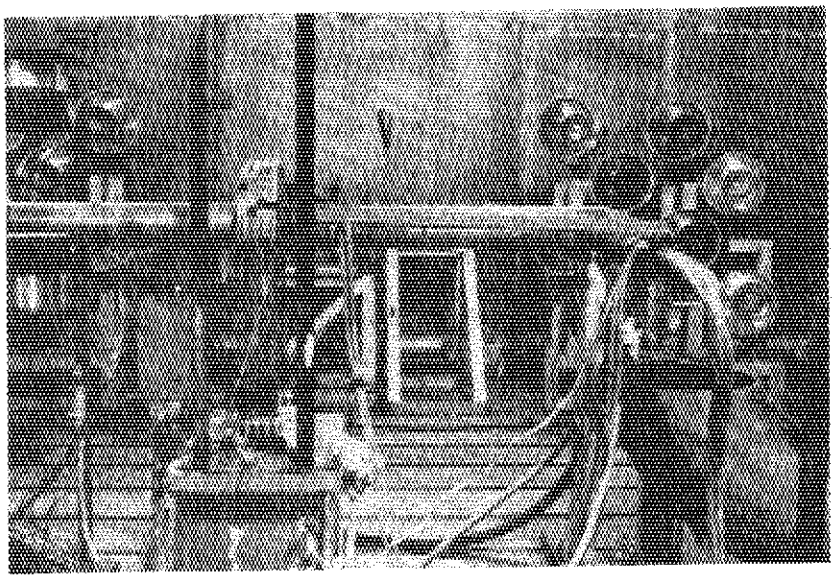

Photo. 3.7.1 RUN 5504 Before the Blowdown

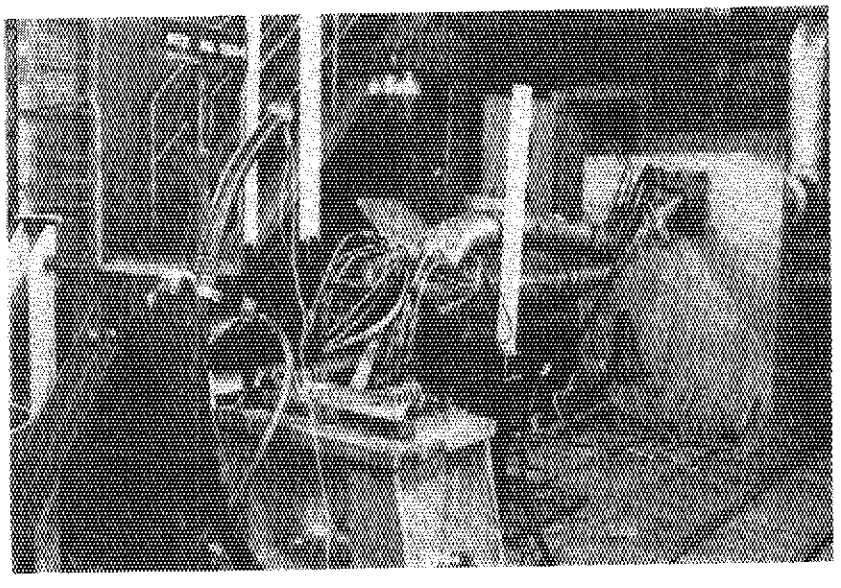

Photo. 3.7.2 RUN 5504 After the Blowdown

4. CONCLUSION

4 inch pipe whip tests (RUN 5407, 5501, 5504, 5603) under BWR LOCA conditions (285 °C, 69 kg/cm^2) were performed with FRPC-II. Clearance of restraint is kept constant at the value of 100 mm and overhang lengths of restraint are parameters 250 mm, 400 mm, 550 mm and 1000 mm. The following results are obtained.

1. It is clarified that the deformations of a pipe and restraints are limited effectively by shorter overhang length.
2. In RUN 5501, the peak restraint reaction force is about 14.5 ton (142.1 kN) at the instance when a pipe collided with its four restraints.
3. In RUN 5504, the plastic hinge is generated in the pipe which collapses and is folded in two around the setting point of restraints.

ACKNOWLEDGEMENTS

The authors wish to make their grateful acknowledgement to Dr. M. Nozawa, Center Director of the reactor safety research center in JAERI, for his valuable advices. Acknowledgement is also due to the members of committee on the Assessment of Safety Research for Nuclear Reactor Structural Components in JAERI (Chairman: Prof. Dr. Y. Ando, University of Tokyo) for their fruitful comments.

4. CONCLUSION

4 inch pipe whip tests (RUN 5407, 5501, 5504, 5603) under BWR LOCA conditions (285 °C, 69 kg/cm^2) were performed with FRPC-II. Clearance of restraint is kept constant at the value of 100 mm and overhang lengths of restraint are parameters 250 mm, 400 mm, 550 mm and 1000 mm. The following results are obtained.

1. It is clarified that the deformations of a pipe and restraints are limited effectively by shorter overhang length.
2. In RUN 5501, the peak restraint reaction force is about 14.5 ton (142.1 kN) at the instance when a pipe collided with its four restraints.
3. In RUN 5504, the plastic hinge is generated in the pipe which collapses and is folded in two around the setting point of restraints.

ACKNOWLEDGEMENTS

The authors wish to make their grateful acknowledgement to Dr. M. Nozawa, Center Director of the reactor safety research center in JAERI, for his valuable advices. Acknowledgement is also due to the members of committee on the Assessment of Safety Research for Nuclear Reactor Structural Components in JAERI (Chairman: Prof. Dr. Y. Ando, University of Tokyo) for their fruitful comments.

REFERENCES

(1) Esswein, G., et al., "Pipe Whip Dynamics - Dynamic Analysis of Pressure Vessels and Piping Components", ASME, 1977.

(2) Miyazono, S., "Fatigue and Rupture Studies of Pipe in Light Water Reactors", Trends in Reactor Pressure Vessel and Circuit Development, Applied Science Publishers LTD, (1980).

(3) Miyazaki, N., Kannoto, Y. and Kurihara, R., "The effect of various parameters on pipe whip phenomena", Vol.21, No.6 Journal of JNS (1979).

(4) Ueda, S., et al., "Pipe Rupture Test Results; 4 inch Pipe Whip Tests under BWR Operational Condition - Clearance Parameter Experiments (RUN 5405, 5406, 5407)", JAERI-M 9496 (1981).

(5) Bathe, K.J., "A Finite Element Program for Automatic Dynamic Incremental Nonlinear Analysis", Report 83448-1, Acoustics and Vibration Laboratory, M.I.T. (1969).

(6) Evans, P.A. Neely, B.B., "Study of the State of Design for Pipe Whip", EPRI NP-1320 (1980).

APPENDIX A Material Property

The tensile test specimen of pipe material is shown in Fig.A.1. These specimens were manufactured from a section along the pipe axis.

The tensile test specimen of restraint material is shown in Fig.A.2. These specimens were also manufactured from a straight portion of the U-bar.

The tensile test result of pipe material's specimen at 285 °C is shown in Fig.A.3. Tensile tests were conducted with Instron Model 1123 Universal Instrument. Proof stress $\sigma_{0.2}$ is 19.6 kg/mm^2 and strain hardening modulus is 380.6 kg/mm^2 from this stress-strain curve.

The tensile test result of restraint material's specimen at room temperature is shown in Fig.A.4. Proof stress $_{0.2}$ of restraint materials is about 37.0 kg/mm^2 from these two stress-strain curves.

These tensile test results are summarized in Table A.1.

Table A.1 Conditions and Results of Tensile Test

No.	Material	Temp.	$\sigma_{0.2}$	σ_u	ψ
1	Pipe	R.T.	29.3	62.8	45.7
2	Pipe	285°C	19.6	46.8	33.5
3	Restraint	R.T.	35.7	60.7	64.2
4	Restraint	R.T.	38.0	60.7	62.2

Note $\sigma_{0.2}$: Proof Stress kg/mm^2

σ_u : Tensile Strength kg/mm^2

ψ : Elongation %

Material is Type 304 stainless steel

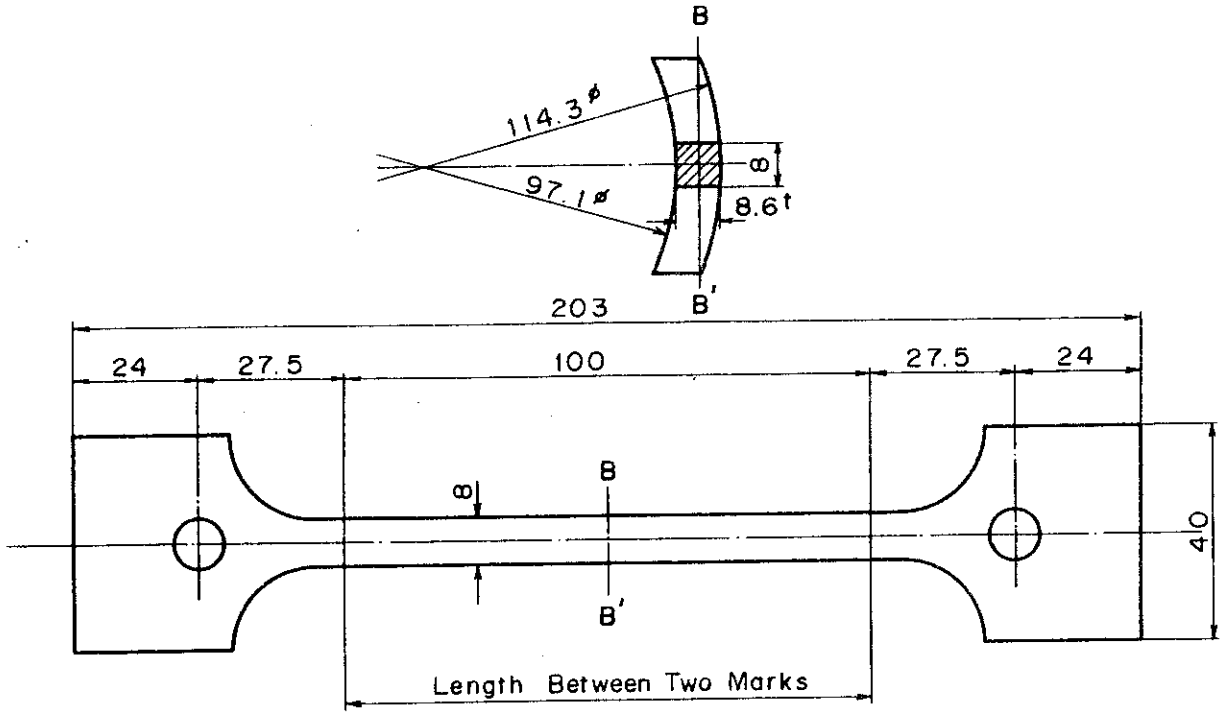

Fig.A.1 Tensile Test Specimen of Pipe Material

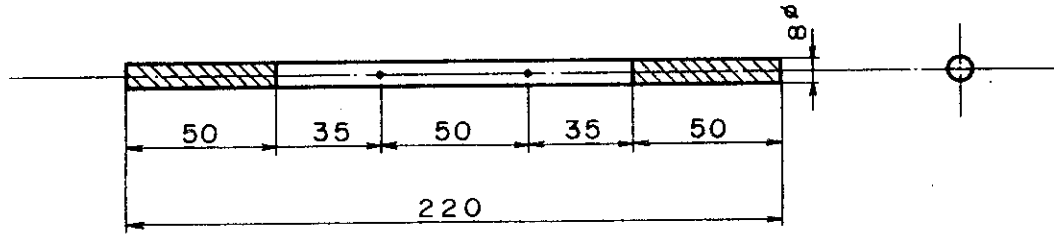

Fig.A.2 Tensile Test Specimen of Restraint Material

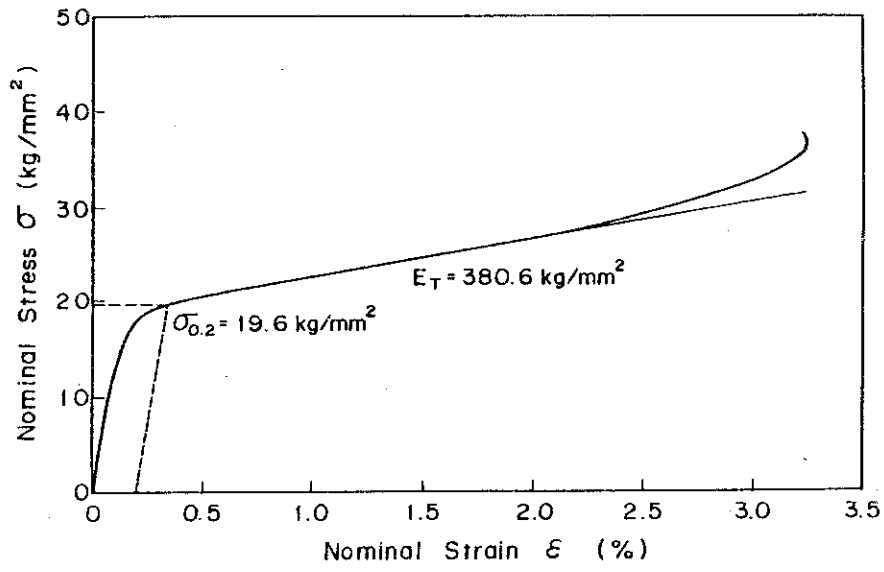

Fig.A.3 Tensile Test Result of Pipe Material's Specimen at 285°C

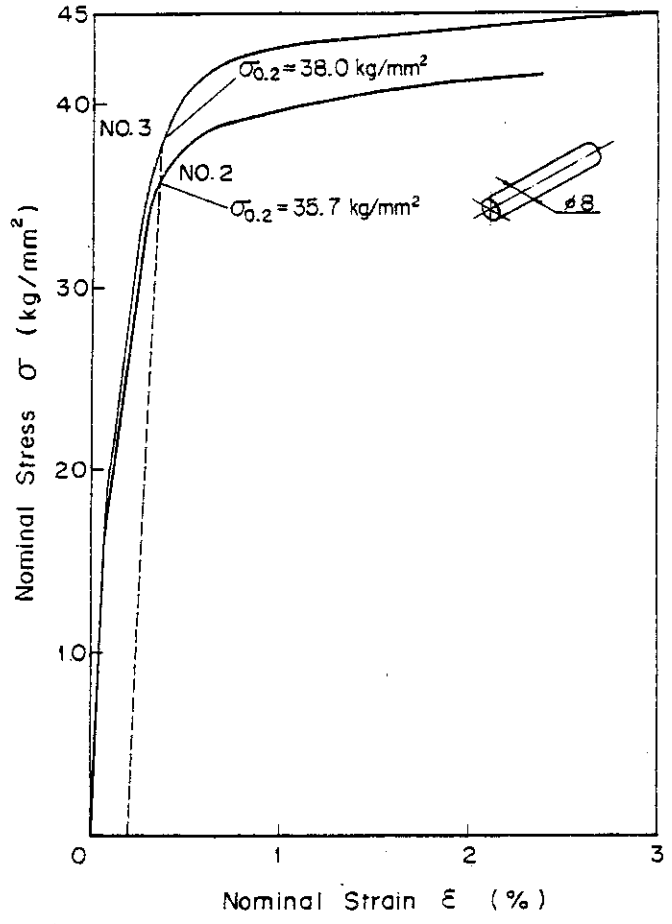

Fig.A.4 Tensile Test Result of Restraint Material's Specimen at R.T.

APPENDIX B Natural Frequency

Mechanical impedance of test pipe is shown in Fig.B.1. It is obvious from this figure that the first natural frequency of pipe is about 7.5 Hz. The vibrator with a impedance head was attached to the free end of pipe. The pipe was clamped at 3000 mm from the free end of pipe to the pipe support. But the fluid was not filled in this pipe and the temperature of pipe is about 15°C.

Mechanical impedance of the restraint system is shown in Fig.B.2. It is obvious from this figure that the first natural frequency of restraint is about 68.0 Hz. The vibrator with a impedance head was attached to the top of U-bar.

Natural frequencies of a pipe and a restraint are summarized in Table B.1. Calculated natural frequencies by ADINA are coincident with those obtained from these tests.

Table B.1 Natural Frequencies of Pipe and Restraint

Freq. No.		1	2	3	4	5
Pipe	Exp.	7.5	53.0	155.0	310.0	480.0
	Cal.	11.5	72.2	202.1	396.1	654.8
Rest.	Exp.	68.0	160.0	410.0	650.0	1100.0
	Cal.	59.5	177.7	384.6	724.7	1136.0

Note: 1. Pipe is a cantilever with a free end and a clamped end.
2. Top of restraint is supported by the vibrator.

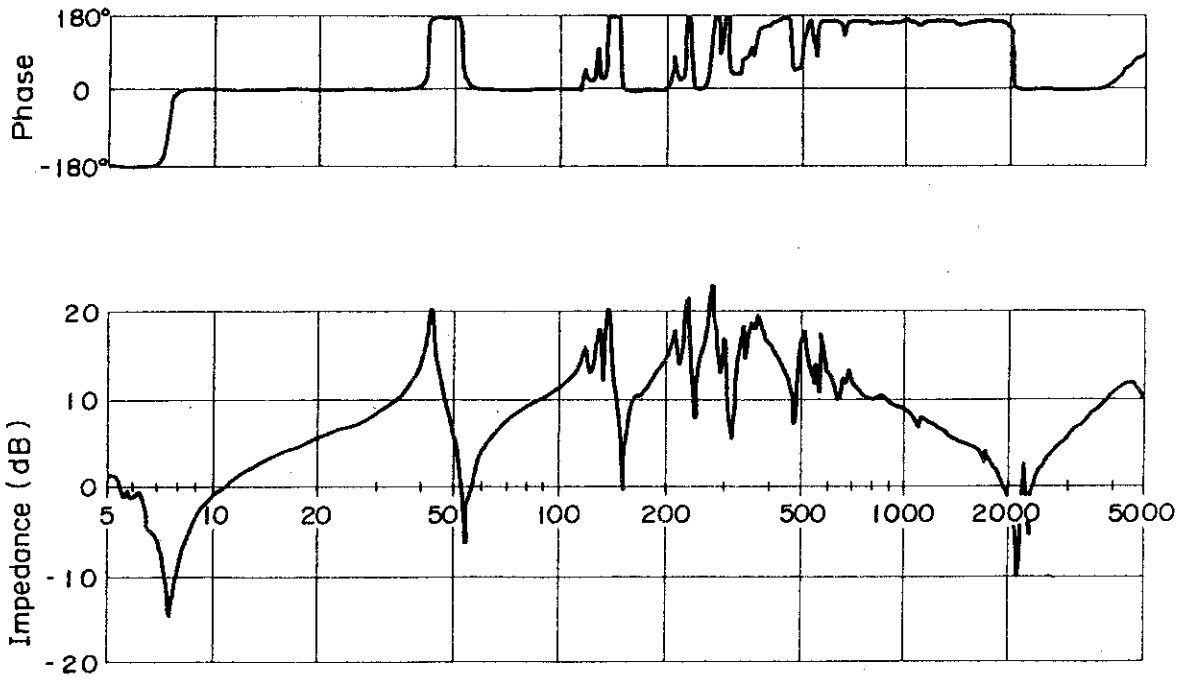

Fig.B.1 Mechanical Impedance of Test Pipe

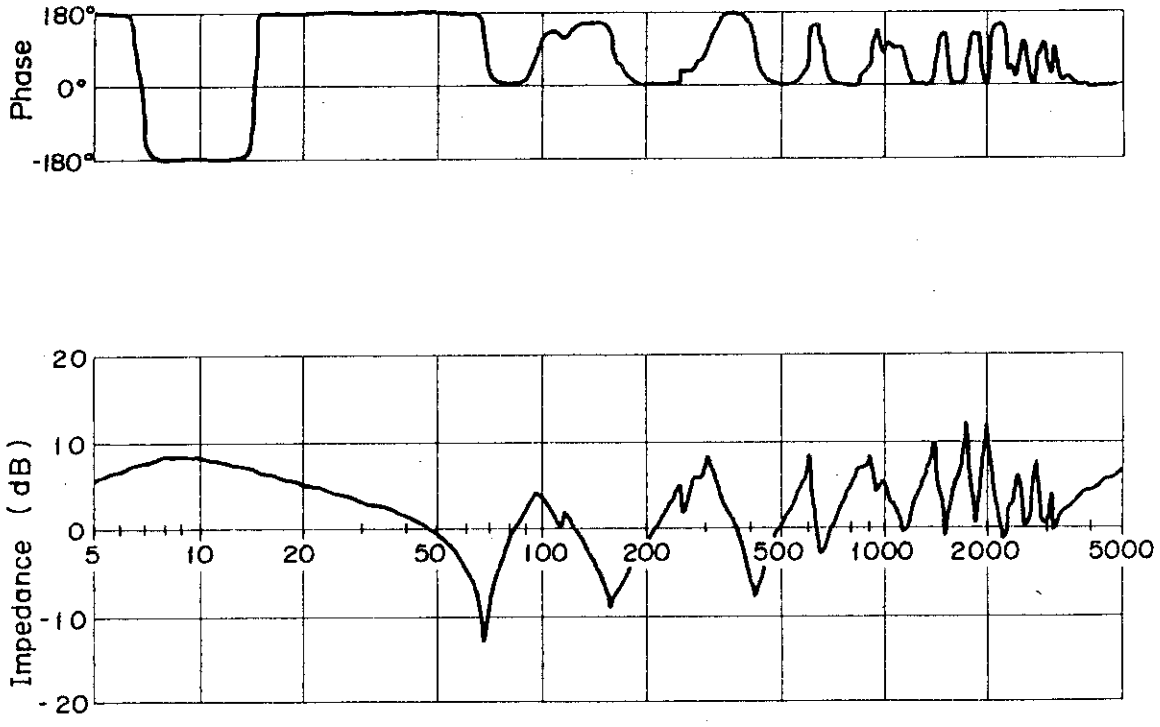

Fig.B.2 Mechanical Impedance of Restraint